September 26, 2000 SRF 000925-09

GRAZING INCIDENCE X-RAY STUDY OF NIOBIUM FILMS

CHESS FEASIBILITY STUDY FS225 PART II

L.N.Hand

Physics Department and Cornell Center For Materials Research

Cornell University, Ithaca, New York

W.R.Frisken

Physics Department, York University, Toronto, Canada

ABSTRACT

The results of Part II of the CHESS feasibility study FS225 are reported. This was carried out with 8.5 KeV x-rays at the F3 beam line. (Part III mainly involved diffuse scattering of 11.0 KeV x-rays at the A2 beam line after the films were bombarded with Ar^+ ions.) Here we report only the F3 results.

Grazing incidence x-ray reflection was studied in three different cases of increasing complexity: a) an epitaxially polished sapphire substrate, b) a 55 nm TaN_2 film on a Si 100 substrate, and c) two niobium films, one annealed and one not annealed.

The rms roughness of the niobium film surfaces was measured to be:

18.78 ± 0.14 $\mathring{A}$ before annealing

20.82 ± 0.15 $\mathring{A}$ after annealing

These numbers and errors were determined by a linear regression analysis of the logarithm of the reflectivity vs. the momentum transfer squared below the critical angle.

Data were also obtained above the critical angle for specular and diffuse scattering. The high Q^2 specular scattering cannot be quantitatively interpreted at the present time, but looks interesting. The diffuse scattering follows a power law, with $R \sim Q^{-1.85 \pm .01}$.

In the future, we will need to link the x-ray results to rf surface resistance and high field flux penetration in the superconducting state. We anticipate that a more extensive measurement at a future date can provide more detailed information on the surface characteristics of niobium films.

In Appendix I, we describe details of the analysis. In Appendix II, we make suggestions for improving the quality of data taken on future runs.

Introduction

Despite many years of study [1, 2], the top 100 nm below the surface of niobium films is not completely understood in terms of all the variables which come into play. Obtaining a better level of understanding is of crucial importance to superconducting rf cavities made with niobium films. Cavities of this type have been pioneered at CERN [3]. The superconducting fields penetrate a distance of order 100 nm beneath the film surface. At high fields, the penetration can be significantly deeper than this, and thus contribute to increased rf losses, if even a small fraction of the field penetrates to the copper substrate.

There is at least a superficial resemblance between the requirements for high quality x-ray mirrors and superconducting rf cavities. In particular, surface roughness is of paramount importance in both cases. A rough surface causes rf losses at high fields due to flux penetration. For a smooth surface, the rf magnetic field is parallel to the surface, and the field penetration is assumed to be governed by $H_{c1} \approx 0.15$T [4]. Any significant roughness reduces the cavity performance in two ways: the flux penetrates at much lower fields [5], $H_{rf} \approx 0.05 - 0.08$ T, and the local electric field is enhanced, causing field emission, and concomitant local heating. Losses will occur for both reasons: fluxon penetration and field emission.

No theory now exists which can quantitatively predict the rf residual surface resistance. However, the BCS resistance is well-understood in terms of diffuse scattering from the surface of the superconductor [6]. We conjecture that the surface also plays a similiarly important role in the residual resistance. Defects at distances below the surface on the order of a penetration depth can also contribute, or even dominate the residual resistance. This includes the "weak link" theory of Halbritter [1]. The structure of a metal film can depend very much on how that film is produced, so there is a possibility for wide variation in the rf properties of superconducting films.

Before concluding surface roughness is an important variable *, we need to study both the roughness and the surface resistance for a number of films.

Assuming surface roughness turns out to be important, we can consider recent advances in making very smooth films on the atomic level. X-ray mirror technology is quite advanced [7]. It could serve as a guide for how we should fabricate rf cavities. As a first step, we have started to evaluate the roughness of some DC magnetron sputtered niobium films prepared at the CCMR Technical Operations Facility. Evaluation of roughness is best done by using grazing incidence x-ray reflectivity [7]. The film is sampled for distances below the surface which can be varied by selecting the angle of reflection.

As part of a "learning curve" for this technique, we measured grazing incidence scattering from a sapphire substrate, and also from a TaN_2 film on a silicon substrate before tackling the niobium films. The first part of this paper consists of a discussion of the data analysis for these preliminary measurements.

* For experimental evidence on this point, see the CERN results [3].

Surface Roughness of a Sapphire Substrate

The sapphire substrate was specified to be "epitaxially polished", so the surface should be smooth on an atomic level[8].

The measurement of reflectivity at very small angles is subject to various systematic geometric and resolution corrections [9]. In Appendix I, we present a discussion of these corrections, which are essential for understanding our data.

We shall usually refer to the angle θ (tilt of the sample) as α to avoid confusion with the detector angle, called 2θ.

In order to compare our data with the theory, we must a) subtract the dark current background in IC3, b) take into account the geometric corrections due to the beam footprint and the detector acceptance, c) account for the finite resolution of the detector.

Two sets of data were taken, located in the files niobe.0609 and niobe.0707. We will analyse the niobe.0609 set first.

We consider a $\theta - 2\theta$ scan which covered the region $-.092 \leq 2\theta \leq 1.008$ degrees. The corrected result for the reflectivity is shown below, together with the best fit to the formula given by Parratt [10] in his landmark 1954 paper. We fit δ, the real part of the index of refraction [11], holding fixed the ratio $\frac{\beta}{\delta} \equiv .0102$ [12].

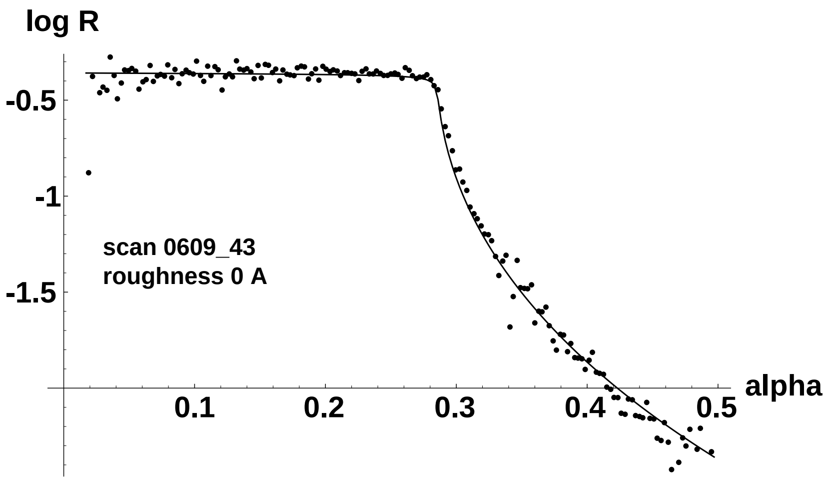

The best fit occurs for a $\delta = 1.243 \times 10^{-5}$. The data fit the theory quite well, but the value of delta is 9.4% higher than the theoretical value, calculated from the electron density in sapphire [13, 14], which is assumed to have a density of 3.928 gm/cm^3. The critical angle from our fit is $\alpha_c = 0.286$ degrees. The critical value of Q, with $Q_c \equiv \frac{4\pi}{\lambda} \sin \alpha_c$, is $Q_c = .0430$ Å^{-1}. The discrepancy between measured and calculated values for the critical angle is .013 degrees. We will discuss possible sources of error below, but the reason for this discrepancy remains a mystery.

After changes in the beam geometry and slit width, we took more distributions into the data file niobe.0707. These include measurements at larger 2θ, out to about 1.5 degrees. The modelling of the beam and detector required more discussion, since some of the important scans were not done. This turned out to be an important procedural mistake, since we must consider the possibility that the beam was not centered in the upstream slits, which were set at a nominal value of 150 microns. In addition, since these slits were scanned vertically in an attempt to increase the intensity, the beam may not any longer be centered on the goniometer center of rotation.

The distribution at larger angles seems to reveal a possible interference dip in the reflected signal at around $\alpha \approx 0.77$ degrees. This could be indicative of a thin (≈ 2.8 nm) dense dverlayer on the sapphire, or it could be of experimental origin.

To calculate the geometric ("footprint") corrections to the raw data, we adopt a different procedure for these data than for the first set of data presented above. We will start by looking at several preliminary scans. In the first distribution, we observe the specular "ridge" by setting $2\theta = 0.520 \pm 0.001$ deg., just below the critical angle, and scanning over α. The figure below for scan 16 reveals that the diffuse scattering is negligible. The integral under the specular peak in the scan 16 figure below is 0.397 (IC3 counts/IC2 count)$\times$degrees. We can use this to see two things: the peak is at a nominal angle of $\alpha = .254$ degrees, so $\alpha_{true} = \alpha_{nominal} + .006$. Also, assuming a reflectivity of 95%, calculated for zero roughness from the Fresnel formula [10], we expect that the integrated amount of beam striking the sapphire is $\frac{.397}{.95} = .417$. If we compare this integral to an integral over 2θ in scan 15 with the sample removed, which gave in the same units 2.13, we can estimate that the fraction of the beam striking the sample when $2\theta = 0.52$ degrees is $2\frac{.417}{2.13} = 0.39$. This is an approximation, which neglects the change in the beam footprint over the width of the scan in α. Finally, we can use the FWHM of .009 degrees and rms width of .0095 degrees to estimate the effective size of the specular ridge at the detector slits. (Includes the effect of finite detector slit width.) From the 2θ scan 15 near zero degrees, there is a FWHM of .019 degrees and a rms width of .011 degrees. These would differ by a factor of two from each other, except for any effects of sample curvature.

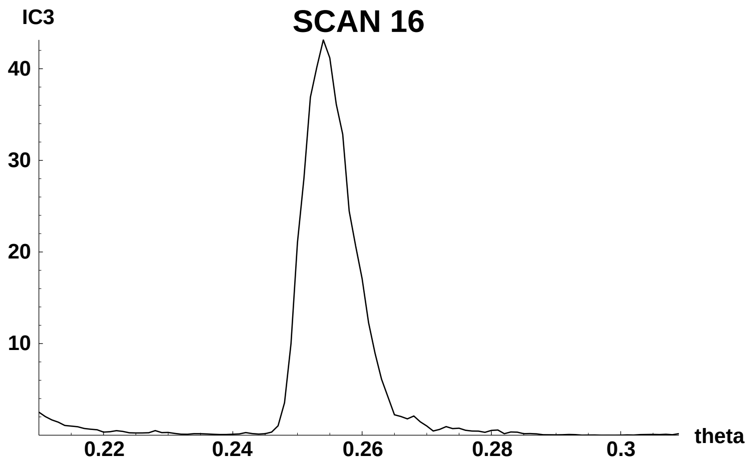

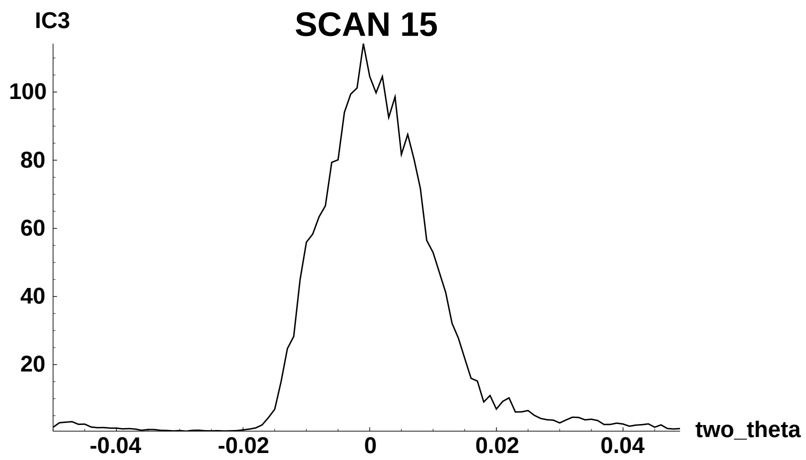

The conclusion that approximately 40% of the beam is striking the sample for $2\theta = 0.52$ degrees is also evident from comparing the peak heights in the two figures above. The projected width of the sample for $\alpha = .26$ degrees is $\mathrm{L}\sin(\alpha) = 45.37$ microns. If we assume a gaussian for the beam at the sample, and that the beam is centered on the goniometer axis, this would imply a sigma for the beam at this point of 45 microns (39.2% coverage). If the beam is not centered on the sample, the sigma must be smaller than this, and the beam offset from the nominal center. This turns out to be the case.

The effective size (for a zero width detector slit) at the detector is $2\mathrm{L}\ \Delta\alpha = \mathrm{L}\ \Delta(2\theta)$. Using the FWHM from either scan 16 or scan 15, with L=0.75 meter, this is an effective FWHM of 236 microns from scan 16 and 249 microns from scan 15. This is the combined effect of scattering, upstream monitor slits, and detector slits. Dividing by 2.3 to get the rms of a gaussian, $\sigma_{total} = 105$ microns. If we represent each slit by a rectangular distribution either w_m (upstream monitor) or w_d (downstream detector), then

$$\sigma_{total}^2 = \sigma_{scattering}^2 + \frac{1}{12}(w_m^2 + w_d^2) \tag{1}$$

Here, we assume the scattering is gaussian. From the integral under scan 15, assuming the Keithley gain for IC3 is 100 times that for IC2 and the ion chambers are identical, we determine the detector slit width to be 278 microns. (The slits were set at ± 150 microns.) Equation (1) above then yields

$$\sqrt{\sigma^2_{scattering} + \frac{w_m^2}{12}} \approx 72 \text{ microns} \tag{2}$$

The effective width of the beam at the detector, corrected for the finite width of the detector slits, is larger than the width at the sample, due to scattering and beam divergence. The beam σ at the sample can only be smaller than or equal to 72 microns, not larger. However, the drastic reduction in the ratio IC2/IC1 by more than an order of magnitude makes us suspect the beam size could be much smaller than this.

All this detective work could have been avoided if the proper scans had been taken! In particular, had we repeated two scans done for the earlier data: a 2θ scan with the detector slits set at 1 mm, and the scan of α with $2\theta = 0$ ("triangle scan"), we would know the beam size at both the sample and at the detector slits.

After scan 16, the value $\alpha = 0.254$ degrees was redefined to be $\alpha = 0.26$ degrees.

We can examine the data from scan 0707-19. This data includes the region below the critical angle. We notice that the data has a strong upward curvature, while the geometric correction is nearly linear in the region $.05 \leq \alpha \leq .26$ degrees. In fact, the geometric correction (fraction of beam in the footprint) curves gently downward in this region, as it must, approaching unity at large angles. The result for a centered beam having $\sigma_{beam} = 45$ microns is compared to the data in the figure below.

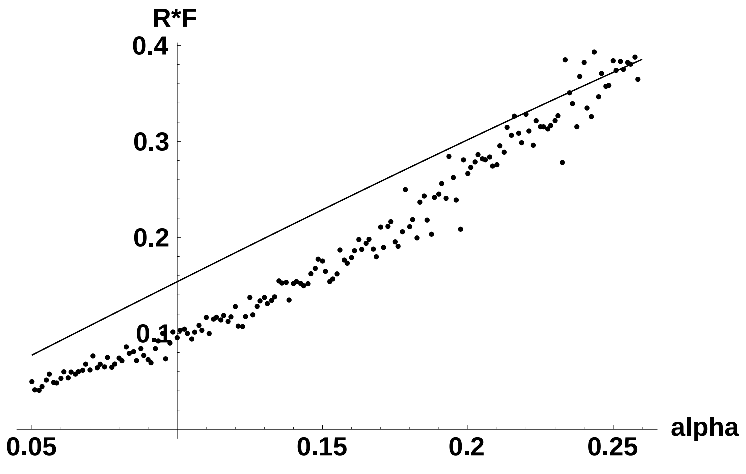

Notice that the figure above is a linear plot of the reflectivity R multiplied by the fraction of the beam intercepted by the sample F. The data have been normalized to 0.4 at $\alpha = 0.26$. The angles shown lie in a region where the reflectivity varies between 99% and 95%. We have assumed R=1 here.

The curvature observed in the geometric correction is not an indication that α and 2θ are not tracking properly, due to a zero offset in one or both of these angles. The data will remain on the the specular ridge if they are on it for one angle, provided the scaling of $\alpha = \frac{1}{2}(2\theta)$ is correct. This is due to the linearity of the relationships at small angles, as is clear from the equation below.

$$v \approx \mathrm{L}(2\alpha - 2\theta) \ - \ h \ + \ \mathrm{dx}\ \alpha \tag{3}$$

We see how sensitively the position in the detector slit depends on $\delta\alpha$. $\delta\alpha = .001$ degree shifts the reflection by 26 microns relative to the slit. Since it is an excellent approximation that v is linear in the angles, a shift of the zero for either one only compensates for h or dx $\neq 0$.

At this point it was realized that the only reasonable explanation for the curvature of the data in the figure above is that the beam is not on the center of rotation of the goniometer. (The sample height was not changed between the two sets of data.) There are two independent quantities which can be non-zero: the center of the beam, which we will call t_0, and the height h of the sample when $\alpha = 0$. Both quantities are measured with respect to the center of rotation of the goniometer. We believe that h=-8 microns for both runs.

The following procedure turned out to give satisfactory results. We selected four points at $\alpha = .05, .1, .2, .26°$, all below the critical angle. Assuming an average reflectivity of 98% in this region, we fitted the log of R*F(α)*B/.98 to the model of a displaced gaussian by t_0 having a rms width σ_0. The log of the beam intensity,$\log B$ is a normalization constant which is fit, so we have 3 degrees of freedom and 4 points to fit.($\log B$ actually includes losses due to curvature and pinholes in the sample film, etc.) The data were taken from the scan 0707-19. The results are shown in the table below. $\log F$ is the log of the fraction of the beam striking the sample. The experimental values and errors are derived by averaging about 30 points taken within .01° in each case.

α	Measured $\log R * F * B$	Calculated from fit
.05	0.683 ± 0.073	0.675
.10	0.992 ± 0.056	1.018
.20	1.422 ± 0.036	1.425
.26	1.579 ± 0.038	1.590

$\chi^2 = 0.12$ for one degree of freedom–indicating an excellent fit.

Attempts to reproduce $\log R * F(\alpha) * B$ assuming a single <u>undisplaced</u> gaussian beam shape were not successful. The initial rise in the intercepted fraction of the beam is thus consistent with a gaussian whose center is located at $t_0 = 15.7$ microns, and with a sigma of only 13.5 microns. The very low intensity (IC2/IC1 =.016) supports this idea. It means that the upstream slits are badly misaligned.

The reader by now must be warned sufficiently that the data presented below are based on the model of a very small beam located above the sample, itself 8 microns below the goniometer center of rotation.

The raw data are presented below on a log scale for $.035 \leq \alpha \leq 1.24$ degrees.

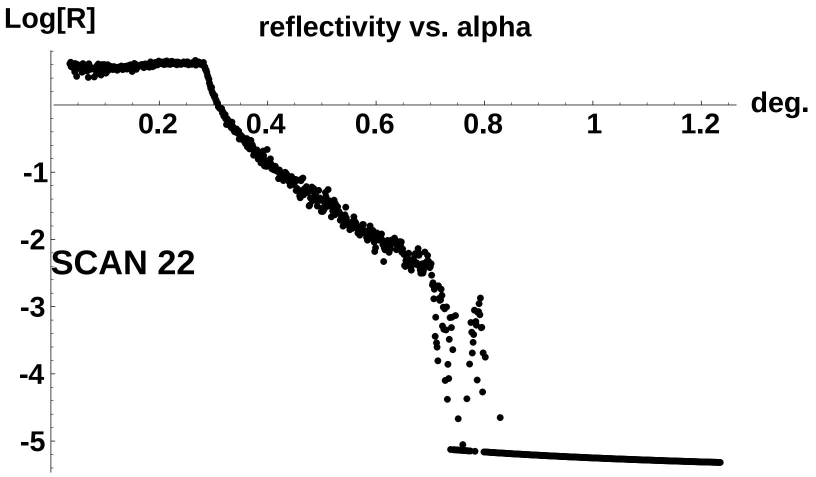

Only the data below $\alpha \approx 0.7$ degrees will be used. This does show our lack of ability to cover a sufficiently wide dynamic range with the detector at hand. The dip at $0.77°$ is possibly an experimental artifact due to improperly zeroing the Keithley amplifier.

A dynamic range of 4 orders of magnitude, extending out to $\alpha \geq 1.2$ degrees is necessary to have roughness sensitivity down to the few angstrom level. The difference between two curves, one with $\sigma_{rough} = 0$ and the other with $\sigma_{rough} = 4$ Å. is a factor of 0.68 at $\alpha = 1.2°$, where the reflectivity is $\approx 10^{-4}$.

;

Fits To Small Angle Data: $0.2 \leq \alpha \leq 0.4$ **degrees**

The data from several runs: niobe.0707-19,22,23 were combined and used for all analyses after this point.

We concentrate on fitting the smallest angles first. The data are first smoothed by convolving the raw data with a gaussian having $\sigma = 0.0025$ degrees. The smoothed data is shown in the figure below as a curve. This amount of smoothing does not seriously distort the curve, even near to the critical angle.

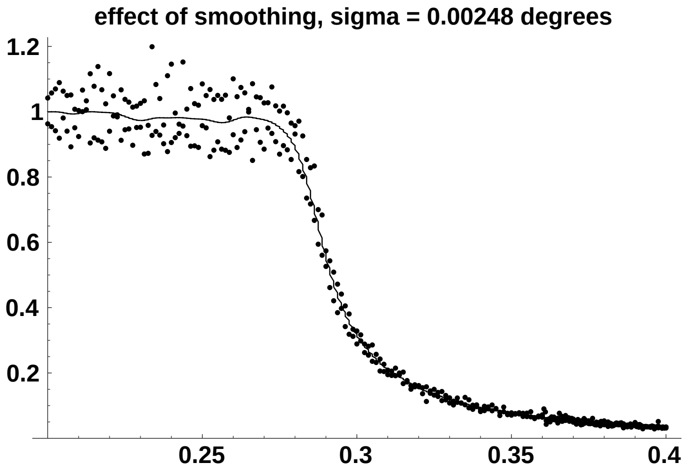

For clarity, we plot the smoothed data again. Note that, in this case, we are looking at a linear scale in the reflectivity.

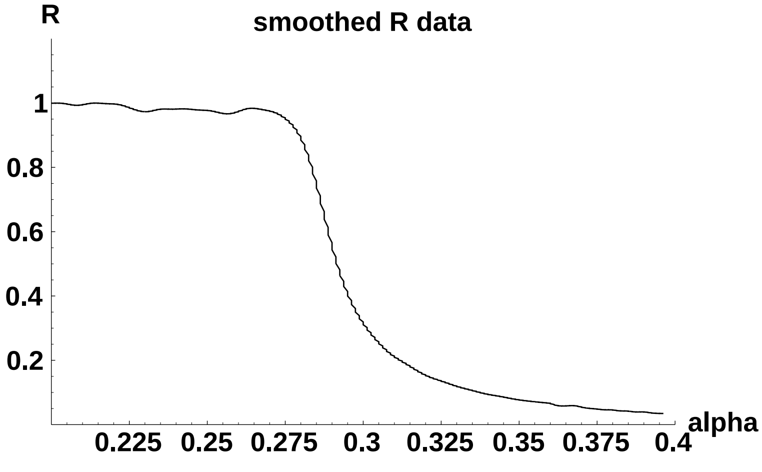

Next we try fitting the data with the theoretical reflectivity [10]. The only input is the value of the real part of the refractive index, δ. (We constrain the imaginary part β to be $\beta = .0102\,\delta$ for all fits. This number comes from Berkeley CXRO calculations[15].) The agreement at angles below the critical angle is very gratifying proof that we have modelled the beam correctly.

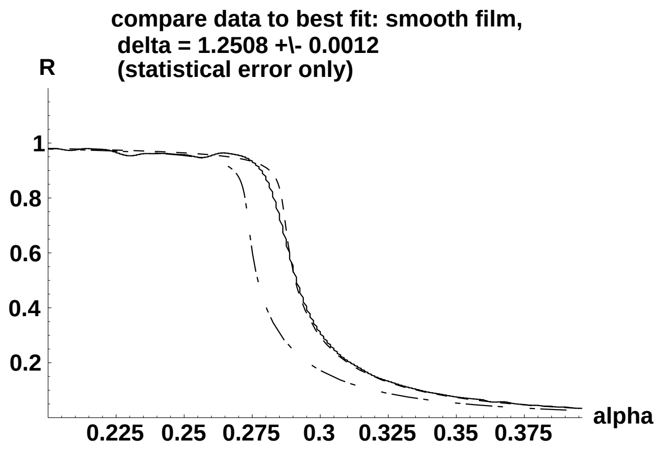

The solid line in the figure above is the data, the line with equal dashes is the best fit to a smooth substrate. The best fit occurs for a value of $10^5\ \delta = 1.2508 \pm 0.0012$(statistical error). This is 11.8% higher than the value of $10^5\ \delta_{calc} = 1.11881$ which is calculated from a sapphire density of 3.928 gm/cm^3. The discrepancy between the calculated value and the best fit value is about 0.016° in α, which is well outside the range of possible systematic error. The fit using the higher value of δ is excellent. We note that the handbook value for the density of gamma-Al_2O_3 is 3.97. If correct, this reduces the discrepancy by 1.0%.

The curve to the left above (dot-long dash-dot) shows the predicted reflectivity for $10^5\ \delta = 1.11881$. The actual surface electron density, with the assumption of a smooth film, must be 11.8% higher than calculations from bulk density[16].

With this result in mind, we tried fitting the recursion formula for a double layer to the data. It is not possible to obtain a value for the thickness, but it must be thicker than about 25 nm. Arbitrarily setting the thickness to 100 nm, we obtain a density ratio of 1.095 as a best fit.

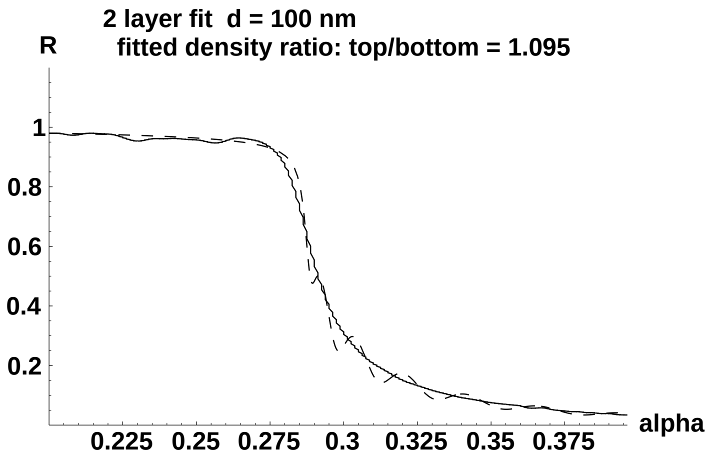

In this case, we see interference “wiggles” from interference between the bottom substrate and the top layer. These would be smoothed over if the electron density varied continously over a layer at least 25 nm thick at the surface.

The slight difference between theory and data right at the critical angle might be explained by two factors not included in the fits: finite resolution of the detector and lack of numerical smoothing of the theoretical curve we compare with smoothed data.

Fits To Log[R] At Larger α

Next, we extend the upper limit on α to $0.7°$. The fit is now done to the log(base 10) of the reflectivity. Using the fit to an infinite substrate obtained above with $10^5\ \delta = 1.2508$, we see below whether it still fits at larger angles.

We begin by comparing the smoothed data(solid curve) with a curve calculated by assuming a single substrate of roughness $\sigma = 0$ (perfectly smooth). The theoretical curve is shown as a dashed line below.

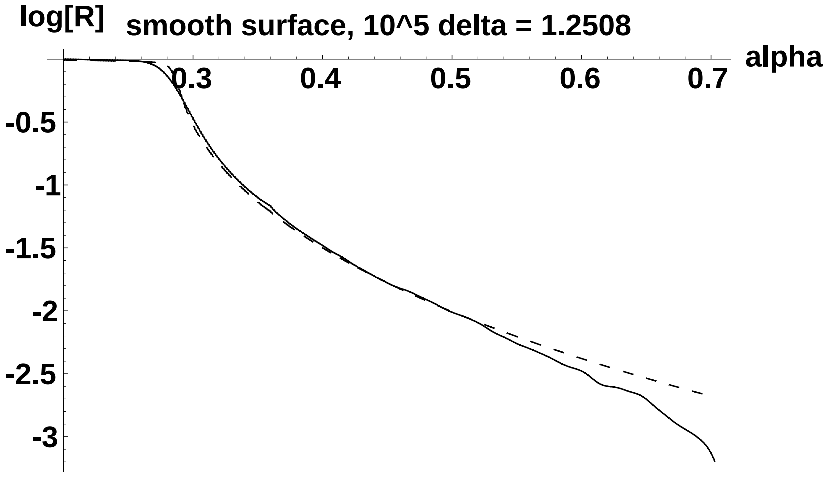

If we assume the surface has instead a roughness sigma $\sigma = 5.83\mathring{A}$ derived from minimizing χ^2, we multiply the data by a form factor $e^{-\sigma^2 Q^2}$. The resultant curve is plotted below (dashed curve), and compared with the data (solid curve).

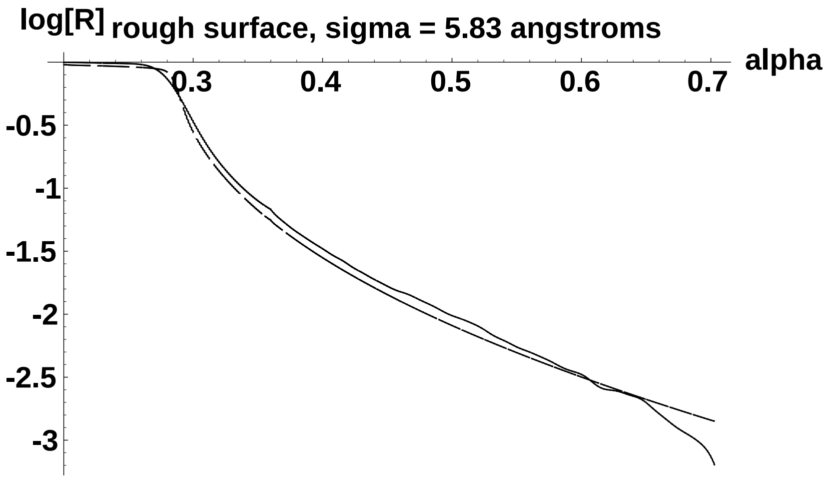

Although the χ^2 is improved using the roughness of 5.8Å, this is clearly not a good fit to the data, as can be seen in the figure above. We can take 5.8Å as a very conservative *upper limit* to the roughness, however. We would need to go to even larger angles, and subtract diffuse scattering to be significantly more sensitive.

Returning to the case of $\sigma_{rough} = 0$, we plot the *difference* between the data and the theoretical curve below:

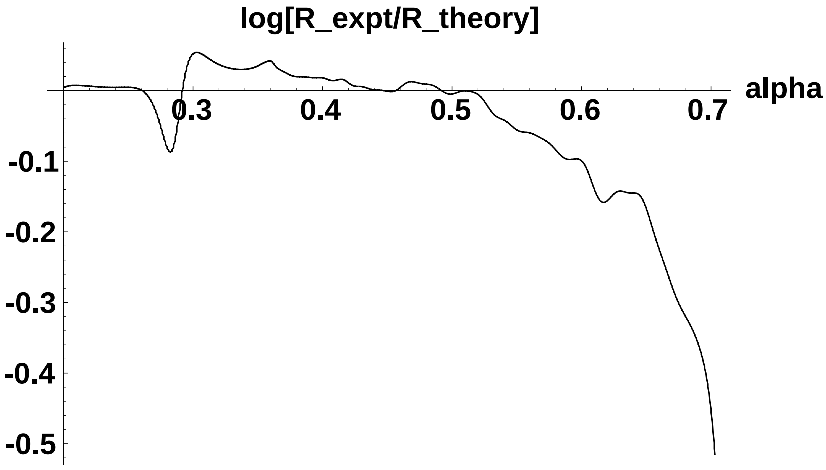

This reveals the systematic differences between the data and the theoretical curve for a perfectly smooth surface. Next, we will briefly consider whether these differences, amounting to only a few percent, except at the largest angles, are possibly due to real physical effects or else just are experimental errors.

Conclusions Regarding the Sapphire Reflection Measurement

It is the lack of a good match between our sample length and the slit size which caused analysis difficulties reported above. For a 10 mm sample length, the detector and beam slits should be no larger than 40 microns. A careful measurement of the beam profile by tilting the sample is essential.

Our second greatest difficulty was controlling the slit widths. A pair of fixed 100 micron slits, together with a 25 mm long sample would have been a major improvement.

We can compare our results with the higher quality data obtained by Gibaud et al [16]. They obtained $Q_c = 0.0405 \pm 0.005\ \AA^{-1}$. For their sample, Gibaud et al measured $\sigma_{rough} = 3.6 \pm 1\ \AA$.

Gibaud et al have measured the reflectivity over 4 orders of magnitude, out to about 6 times the critical angle, something we were not able to do with the F3 diffractometer.

We conclude that the anomalous surface density as measured here by us, if correct, means that we need to understand the surfaces of our sapphire substrates better, since this will affect the quality of niobium films deposited on them. We might start by comparing different samples from different sources. A LEED or RHEED study of the surface could also be done.

Study of a Titanium Nitride film on 100 Silicon *

From the Berkeley CXRO data, we can tabulate the real and imaginary parts of the complex index of refraction. The RBS revealed that our film was chemically TaN_2. We have calculated δ and β for a nominal density of 10 gm/cm^3. These can be scaled when the actual density is determined from the x-ray measurements.

Calculated Complex Index Of Refraction For 8.5 KeV X-rays

Material	Assumed Density	$10^5\ \delta$	$10^6\ \beta$
Si	2.33	0.681074	0.139452
TaN_2	10	2.22611	1.39113

The RBS results are shown in the figure below.

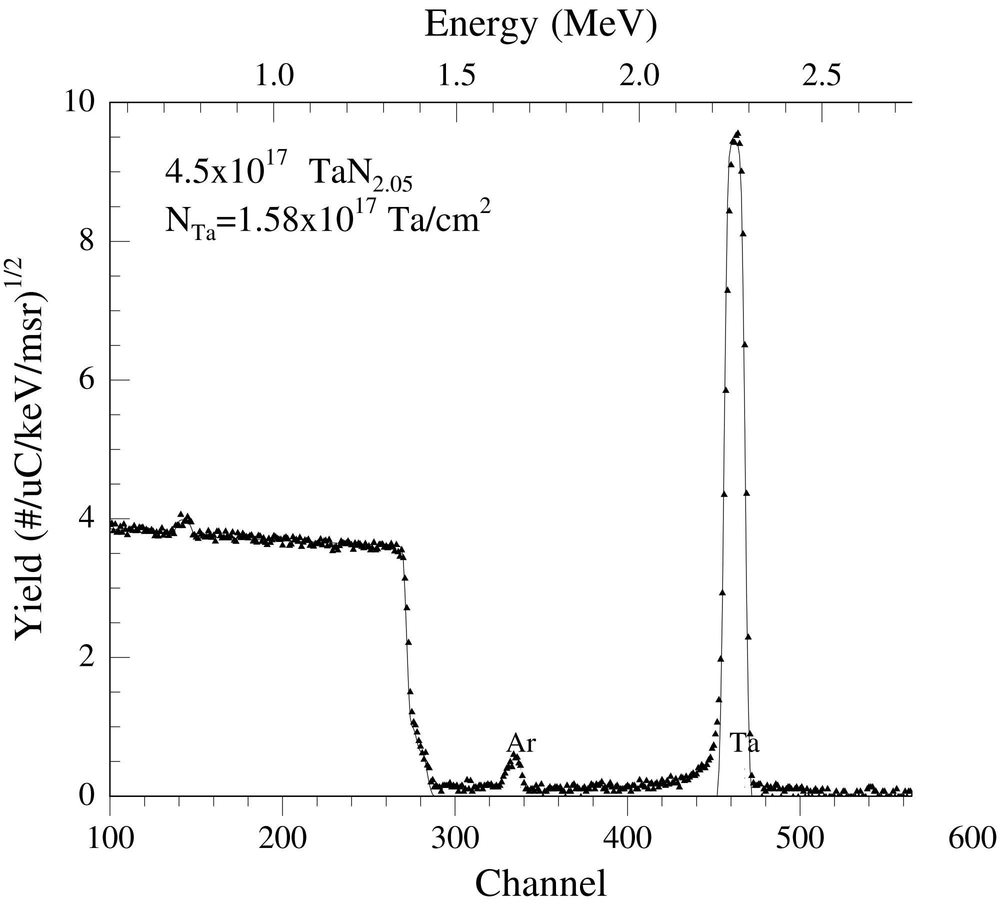

There are several notable features in the RBS data. The ordinate is the square root of the number of

* sample #2267

counts. This is done in order to render small effects visible. The bump at channel 330 is caused by argon trapped in the film at the below 1 percent level. The other bump at channel 120 on top of the silicon continuum is due to the nitrogen in the TaN_2 film. The boundary between the TaN_2 and the Si is very sharp on the nanometer scale.

Using the Alpha-Step apparatus, we measured an approximate film thickness of 65 nm. This would imply a TaN_2 film density of 8.4 gm/cm^3. However, the x-ray results, in combination with RBS, will yield much greater precision for both the density and the thickness.

Using this nominal density to scale the value of δ in the table above, we estimate the x-ray critical angle to be $\alpha_c(estimate) \approx 0.35$ degrees.

We follow the same general procedure we used on the second set of sapphire data discussed above. Here, however we do have a "triangle" α scan tilting the film while keeping 2θ set at 0. Also, we have an earlier scan of 2θ without any film in place. From this latter scan, we learn that $w_d = 232$ microns. The sigma of the 2θ scan is 91 microns, hence the beam sigma at the detector is 61.7 microns. This is the sum of scattering plus instrinsic beam width plus the effect of any beam divergence. The triangle scan yields the values $L_s = 21.7$ millimeters, $dx = 1$ millimeter and $h = 11$ microns.

As a check on our beam model, we compare the specular scan for 2θ =0.600° with the straight-ahead scan. In both cases, we take the integral, multiplying by 2 to take into account $2\theta = 2\alpha$. We obtain

$$R(.300°) * F(0.300°) = 2 * \frac{\int I(2\theta = 0.6)\ d\alpha}{\int I\ d(2\theta)} = 2 * \frac{.0.774}{2.76} = 0.56 \tag{4}$$

If we assume $R = 0.815$, we deduce the beam fraction in the sample footprint for $\alpha = .3$ is 69%.

As before, we form a table for various small α of the $\log\frac{IC3}{IC2} = \log[R * F * B]$, and try to fit a displaced gaussian of unknown width and displacement. We correct for the x-reflectivity of a TaN_2 film having a density of 8.4 gm/cm^3.

α	Measured $\log[R * F * B]$	Calculated from fit	Calculated beam fraction F
.05	1.11 ± 0.23	1.15	0.183
.10	1.48 ± 0.05	1.48	0.387
.20	1.79 ± 0.05	1.78	0.768
.26	1.82 ± 0.06	1.85	0.906

From the same model,as a check, we calculate that $F(.30) = 0.956$.

Below is a table of parameters used in the modelling of the beam footprint:

Parameter	Symbol	Value used	Unit
sample length	L_s	14.6	mm
sample height	h	-3.5	microns
sample displacement	dx	0.8	mm
beam height	t_0	13.9	microns
beam sigma	σ	14.64	microns
Log[B] (see text)	$\log B$	1.89	—

If we can believe the gain ratio on the Keithley amplifiers and that the ion chambers IC2 and IC3 are identical, $B_0 \approx 100, \log B_0 \approx 2$ if the entire beam is detected when $2\theta = 0$. The *effective beam ratio* B includes many corrections and is $B \leq B_0$.

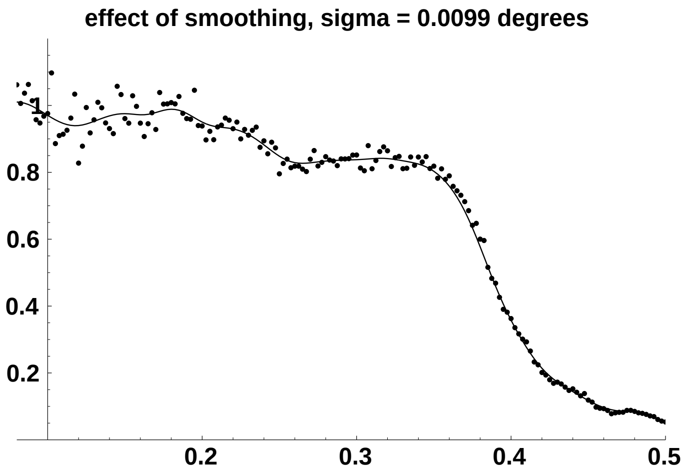

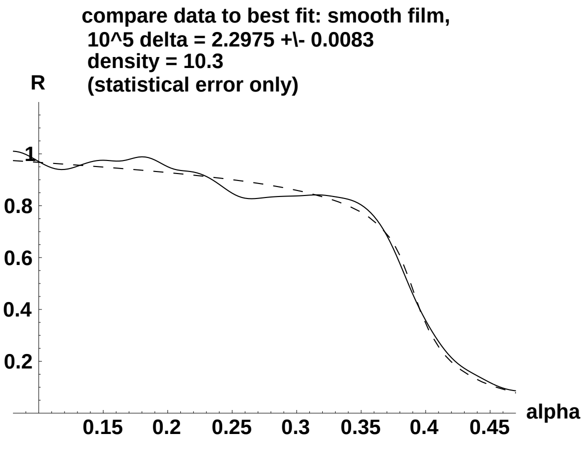

Can we believe the fluctuations observed at $\alpha < 0.2$ in the data above are real and not experimental artifacts? It would take considerably more work to be certain of the answer to this question. But we can ask a different question: is it physically possible to observe a real effect of this kind?

TaN_2: Fits To Log[R] At Larger α

The smoothed data for $0.1 \leq \alpha \leq 1.87$ degrees is shown below.

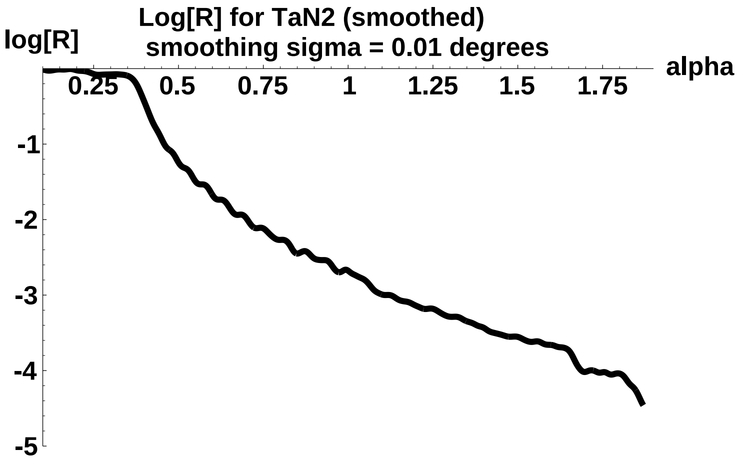

We have measured 4.5 orders of magnitude in the reflectivity! The interference between the TaN_2 film and the Si substrate is visible in the region $\alpha \approx 0.75°$. We will present more data taken in this region below.

Taking the values for the TaN_2 δ, β from the small angle fit ($\alpha \leq 0.47°$), we plot the curve for a single infinitely thick film of TaN_2. In addition, we minimize χ^2 by allowing a roughness "form factor". The result is shown in the figure below:

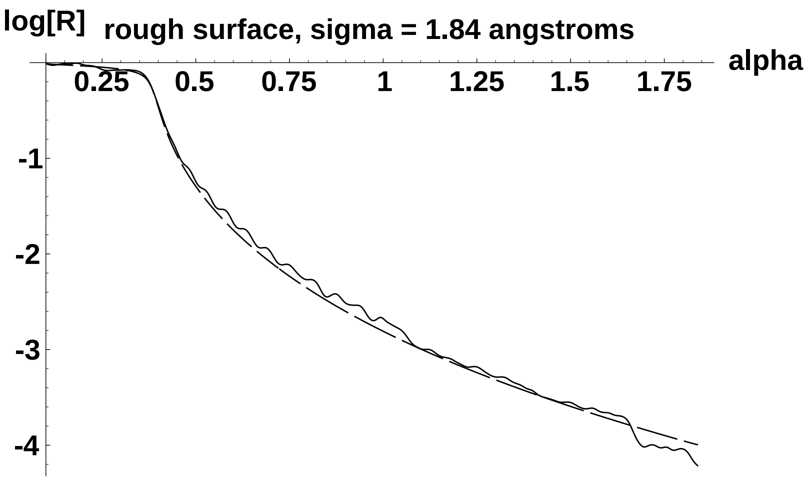

The difference between the data and the fitted curve, which was smoothed just like the data and which does not allow for the underlying Si substrate gives a closer picture of the correspondence between the theory and the data:

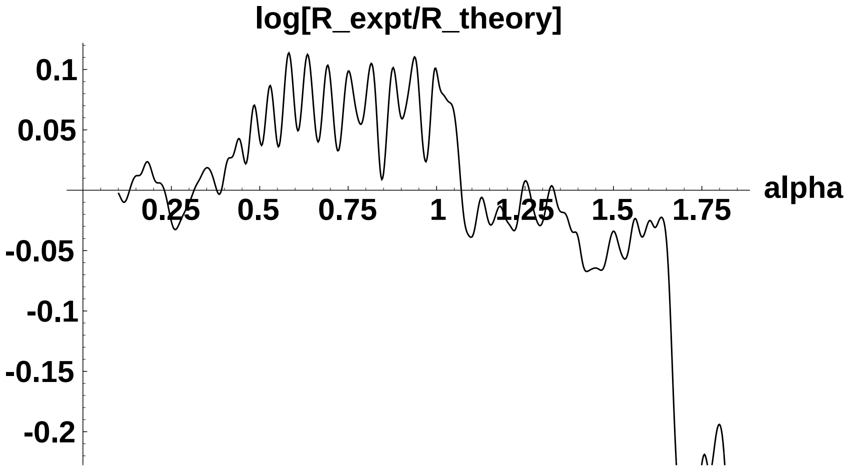

It is remarkable that, with a roughness of only 1.8Å , the two curves agree within 10% almost over the whole range of angles and over 4 decades in R. The effects of interference between TaN_2 and Si are more clearly visible in the difference plot.

To study this interference more closely, and obtain the film thickness, we turn to another set of data which concentrates on the region of maximum interference.

The smoothed data is shown in the figure below. This was a long run which concentrated on getting a large number of counts at each point.

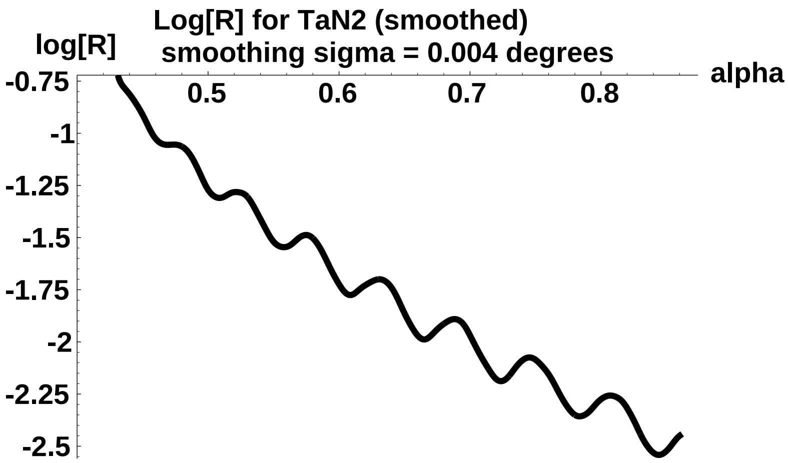

We attempted to fit these points with a 2 layer model, assuming the bottom layer was silicon. In the fit we varied the thickness of the TaN_2 film and the ratio of the actual density to 10.3, which was determined by fitting the critical angle as explained above. The best fit is shown below:

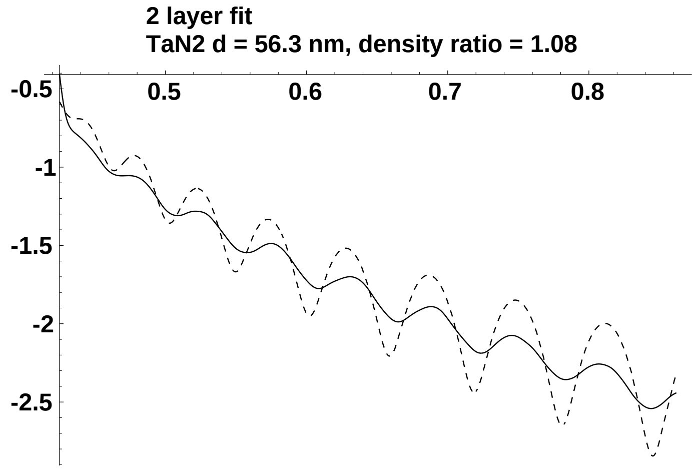

The comparison between the theoretical curve and the data is extremely sensitive to the thickness of the film. A change as small as 0.5 nm is easily detected. Using the RBS results and the new value of the film thickness of 56.3 nm, we recalculate the density to be 9.7 gm/cm^3, now within 6% of the value 10.3 determined from the critical angle measurement. The additional density increase above 10.3 of 8.5% assumed for the fit above has the effect of increasing the theoretical curve and improving the agreement with the data. This is not consistent with the critical angle result for a single layer of TaN_2, however.

Something is causing the amplitude of the interference peaks to be suppressed. It is most likely due to small variations in the thickness of the tantalum nitride film.

We can take into account possible variations in the thickness of the TaN_2 film by introducing a complex form factor into the Parratt expression for the multilayer reflection recursion formula. We assume a gaussian distribution around an average thickness d with sigma σ_{12}. The form factor multiplies the a^4 in Parratt's expression [10] for $R_{n-1,n}$ (equation 8). It is

$$Exp[-\frac{f^2}{2}\left(\frac{4\pi\sigma_{12}}{\lambda}\right)^2] \tag{4}$$

with

$$f \equiv \sqrt{\alpha^2 \;-\; 2\delta \;-\; 2i\beta} \qquad Im[f] < 0 \tag{5}$$

Although this greatly improved the fit, there are obvious systematic variations between the theoretical curve and the experimental data. This means that the thickness variation cannot be the whole explanation. It does provide an upper limit to the thickness variation of $\approx$ 2 nm, however.

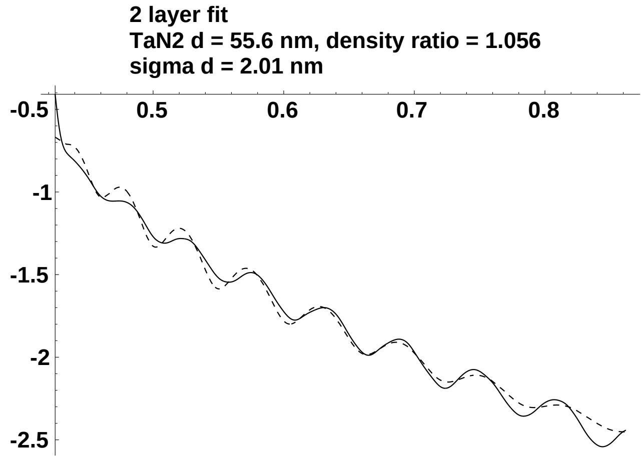

Two nanometers is an overestimate for σ_{12}. What other effects could be present here?

What we have estimated above could be called the effect of "*coherent* thickness variation". By averaging the amplitude before squaring and taking the log, we are calculating the effect of a variation in thickness of the film over a distance over the film surface of order the transverse coherence of the x-ray beam divided by α, which we guess is a distance like 100-200 microns. There is, of course the *incoherent* effect of summing the reflectivity over thickness variations in more distant parts of the film. To do this properly and do a least squares fit would take more programming effort than we are prepared to do at this point. So we present the curve for this additional average, assuming a sigma $\sigma(incoherent) = 1.5$ nm. A slightly surprising result is that a better fit would cause us to decrease the calculated film thickness by a few nanometers.

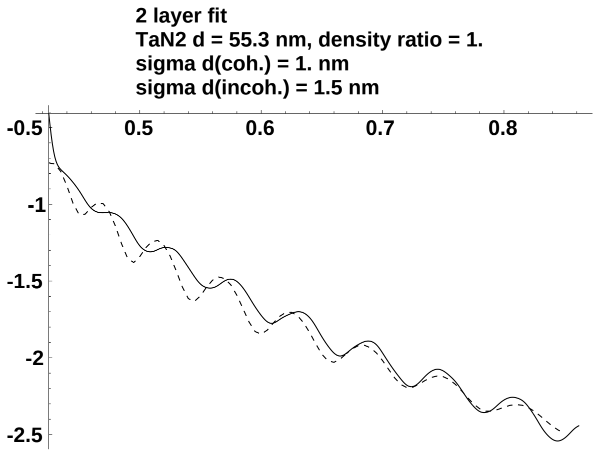

We have achieved our original objectives. The film density is 10.3 gm/cm^3 with an error of $\pm 6\%$. The lower limit is given by the RBS results, in combination with the thickness. The upper limit is given by comparing the reflectivity at $0.425 \leq \alpha \leq 0.85$ degrees with the critical angle from the smaller angle data. Any discrepancies can be due to errors in the beam modelling, which affect the small angle data. The film average thickness is 55.3 ± 0.3 nanometers, the error being derived from the fit. The additional variation is not an error, but a physical reality: $\sigma(coherent) \approx 1$ nm, $\sigma(incoherent) \approx 1.5$ nm.

More data was taken to look at the details of one of the interference fringes. If we wanted to go further in the analysis, we could use this to study the film structure in more detail. For example, we could look into a possible variation in film density over the film thickness. We present it here because we can't resist showing the high quality of this data.

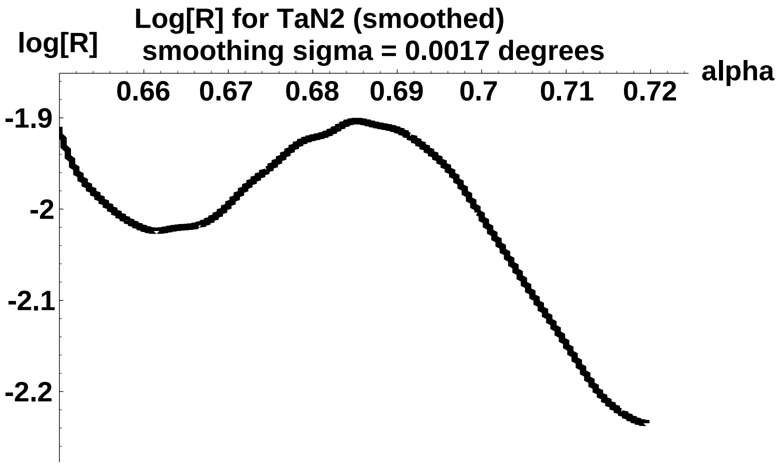

Based on fluctuations between 3 different runs, there is an overall normalization error of 2%. This is the statistical error and does not include any systematic errors in the normalization.

Study of Two Niobium Films: Annealed and Unannealed

For obscure reasons, the slit widths and beam geometry were changed before the niobium film data was taken. Therefore, we must begin all over again to understand the parameters of the beam.

We start by considering the "zero scan". The area under the peak, and the peak height give us a measure of the detector vertical slit width, which was not recorded. The upstream (monitor) vertical slit was nominally 450 microns. The ratio IC2/IC1 was typically .092, so a much higher percentage of the beam is accepted than for the TaN and sapphire data. The results of this scan are tabulated below.

file-scan #	niobe.0708-33	
area under peak	0.0345	IC3 counts-degrees/IC2 counts
observed peak height	1.29	IC3 counts/IC2 counts
" FWHM	.026	deg.
calculated detector slit width w_d	350	microns
observed rms $\sigma_{2\theta}$	.0114	deg.
calculated rms= fwhm/2.3	.0113	deg.
estimated peak, gaussian approx.,area+rms	1.22	IC3/IC2
upper limit to $w_d \leq \frac{\sigma_{2\theta}}{\sqrt{12}}$	513	microns

We will assume $w_d = 350$ microns.

Next, we did a "triangle scan" after adjusting the sample height to intercept approximately 50% of the beam. The niobium film sample was 13C, which was the unannealed sample. From this we can obtain $h - t_0$ and dx, the sample height from the beam. There is some information about the beam size also. We must assume the sample length $L_s = 9.95$ mm, which was determined by measurement with a micrometer. (9.9×10.0 mm) We tabulate the results of the triangle scan below

file-scan #	niobe.0708-36	
area under peak	0.656	IC3 counts-degrees/IC2 counts
peak at α	-.06	degrees
observed peak height	0.605	IC3/IC2
" FWHM	1.02	deg.
observed rms σ_α	0.544	deg.

As the figure below shows, the shape was an almost perfect triangle.

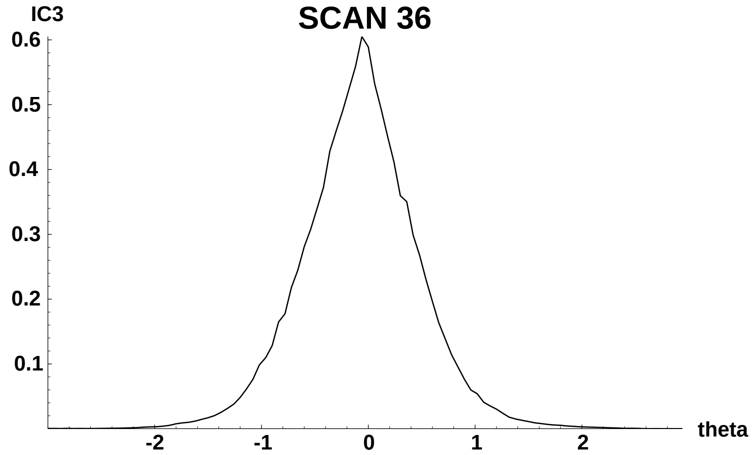

Assuming that the distribution of the beam is a gaussian, we can fit the slopes of the left and right sides to determine σ for the beam, dx and by comparing the peak intensity with the peak from the zero scan, obtain $h - t_0$ as well. The table below summarizes the results.

I_0	1.02	zero scan peak
$I_\alpha(peak)$	0.605	triangle scan peak
initial slope (left-right)	$\frac{.398 I_0 \ L_s}{\sigma}$	
from fit, $\sigma =$	57.3	microns
“ ”, $dx =$	-0.20	mm
“ ”, $h - t_0 =$	-13.5	microns
“ ”, peak at $\alpha =$	-.0489	deg.

We will return to the interpretation of σ shortly, but first we examine another scan: a “specular scan”, the results of which are shown below:

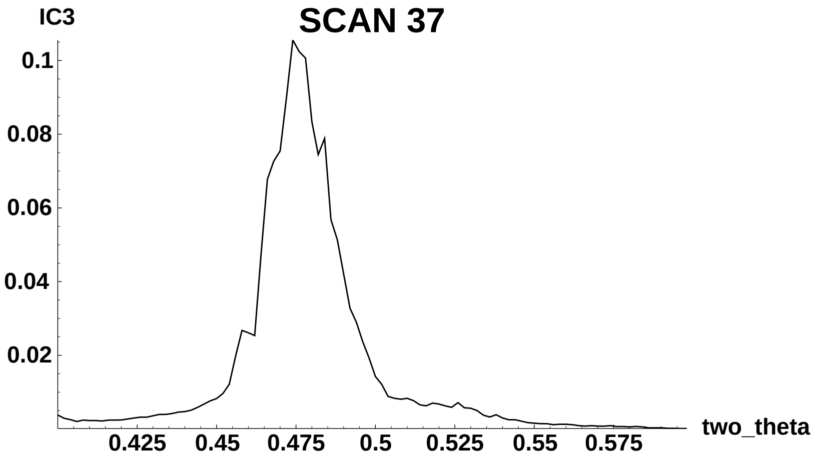

The area under this scan is taken without correcting for the small amount of diffuse scattering visible above. It is .00306 cts*deg/ct. The ratio of this area to the zero scan area of .0345 in the same units is:

$$\frac{2\theta \text{ scan area}, \alpha = .24^\circ}{2\theta \text{ scan, nosample}} = 0.0887 = RF\frac{B}{B_0} \tag{6}$$

As before, $R(\alpha)$ is the reflectivity, F is the geometric fraction of the beam and $\frac{B}{B_0} < 1$ is a correction factor for the "effective" beam intensity for 100% reflectivity.

To calculate F, we need to model the beam. The $\sigma = 57.3$ microns found from the "triangle" scan is a combination of the beam rms width and the detector. If the detector were a gaussian, then

$$\frac{1}{\sigma^2_{beam}} + \frac{1}{\sigma^2_{detector}} = \frac{1}{\sigma^2} \tag{7}$$

Making the approximation that $\sigma_{detector} = \frac{w_d}{\sqrt{12}}$, we estimate $\sigma_{beam} = 69.5$ microns, a much larger beam vertical height than previously used. Assuming this, and a gaussian approximation for the beam, we calculate F$=$ 0.228, hence

$$R\left(\frac{B}{B_0}\right) = 0.389 \tag{8}$$

Further dividing by the theoretical reflectivity for niobium * having a smooth surface, $R_{theory} = .914$, we obtain

$$\left(\frac{R}{R_{theory}}\right)\left(\frac{B}{B_0}\right) = 0.425 \tag{9}$$

This number, equation (9), differs from 1 only because a) the niobium surface is rough, and/or b) the effective beam after reflection is not equal to the incident beam.

Next, we look at a simultaneous $\theta - 2\theta$ scan, extending almost to 2θ =2 degrees. This is our raw data for the niobium film 13C:

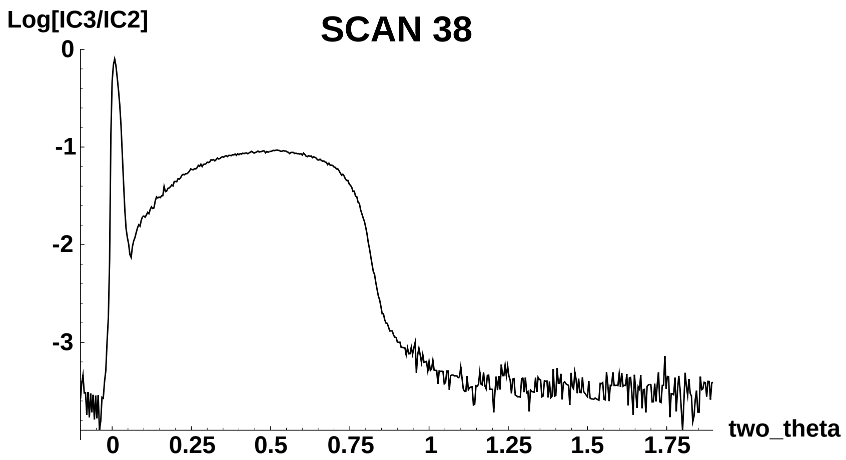

* We used $10^5\delta = 2.1643$ and $10^6\beta = 1.2068$, from Berkeley CXRO calculations.

We remove the geometric correction of F from the data, and plot the Log[R] up to a constant factor (to be determined) over the angular range $.03 \leq \alpha \leq 0.948$.

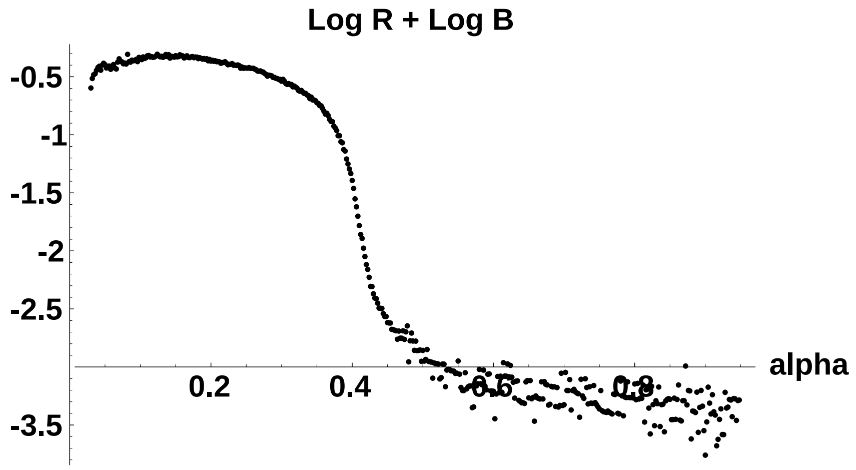

Above about $\alpha = .42$ degrees, the data falls less rapidly than the theory for specular reflection predicts, even for a smooth surface! This means that we no longer have specular reflection, but are in the regime of diffuse reflection instead.

An even more interesting plot results when we divide out the theoretical prediction for R, and plot the Log[R/R_{theory}] (still with an arbitrary additive constant Log[B]) vs Q^2. A roughness form factor will give a straight line here.

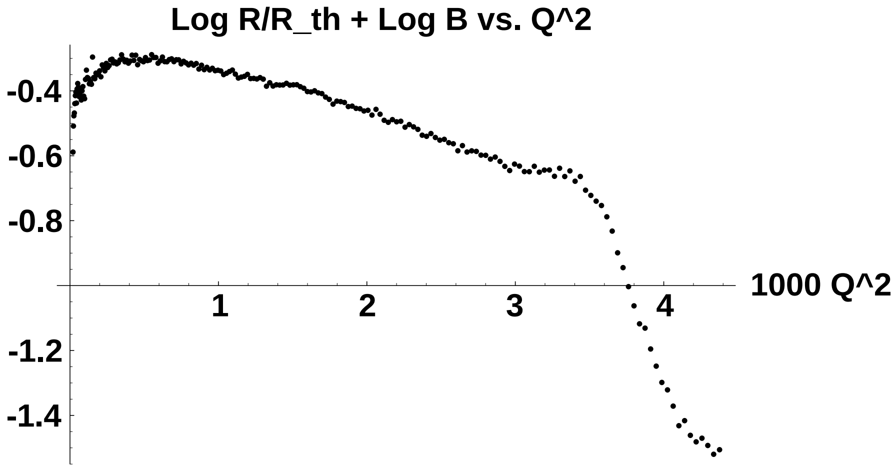

The critical angle, $\alpha_c = 0.377$ degrees. This corresponds to $1000\ Q_c^2 = 3.21$. By fitting a straight line to the data above, over the range $1 \leq 1000\ Q^2 \leq 3$, we find

$$\sigma_{rough} = 18.78 \pm 0.14\ \mathring{A} \qquad log[B] = -.165 \pm .004 \qquad B = 0.68 \tag{9}$$

The errors were obtained by linear regression, fitting the data in the region $1 \leq 1000\ Q^2 \leq 3$. The discrepancy at very low Q^2 is due to inadequacies in our model of the geometric correction fpr the beam footprint, which appears to be in error by up to 20% at these very small angles. The correction becomes very large at very small angles, so this error is not surprising, given the large beam size.

The very good fit to the theory after a "roughness form factor" is added is shown below. The dotted line compares the higher Q^2 region ($1000\ Q^2 \geq 1$) with a theoretical curve which includes the form factor.

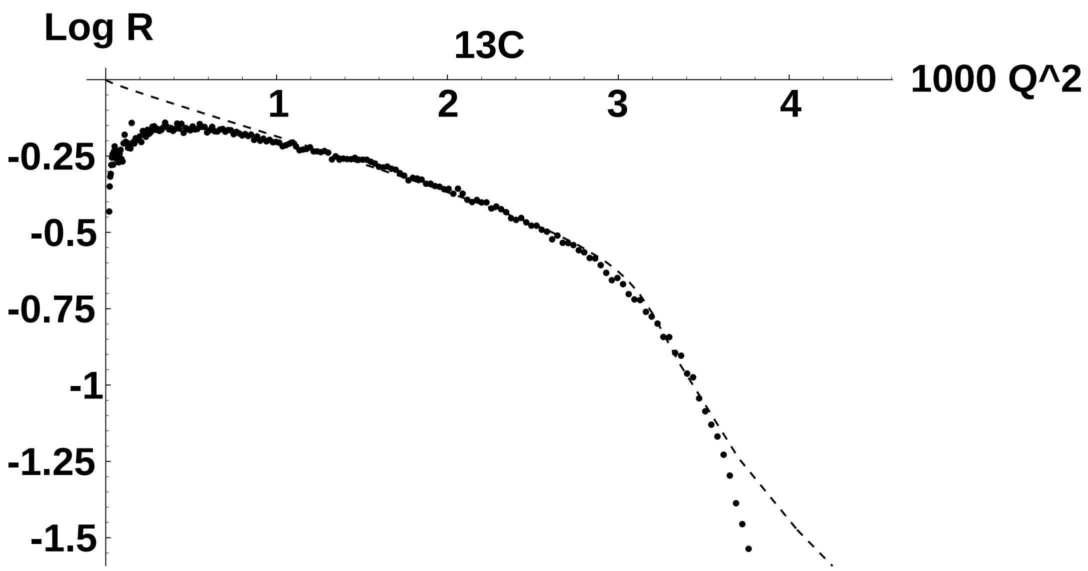

For $1000\ Q^2 > 3.6$, the experimental curve falls more rapidly than the theory. The rate of fall also fits a straight line, with a $\sigma = 55\ \mathring{A}$. This more rapid falloff must indicate some kind of inhomogeneity below the film surface. This could be a very important part of our data, but we do not know how to interpret it. The region below the surface is only probed if the angle is greater than the critical angle. At even higher $1000\ Q^2 > 4.2$, the reflectivity flattens out and falls less steeply than even the theoretical curve for a smooth surface and homogeneous film. We assume this is due to diffuse reflection, which we will discuss separately below.

We now proceed to analyze the annealed film 13D.

We will not describe the analysis in detail, since it was exactly the same as for 13C, with two important differences: the Keithley gain was on the 10^{-10} scale for the $\theta - 2\theta$ scan, an increase of three orders of magnitude beyond the 10^{-7} scale used for film 13C and for the preliminary scans on film 13D. The beam width inexplicably changed to 150 microns from 70 microns, causing the geometric correction to be even larger at the smaller angles. The change was probably due to a slight shift in the beam position on the upstream slits. The results are shown below in a series of figures.

First, the raw data:

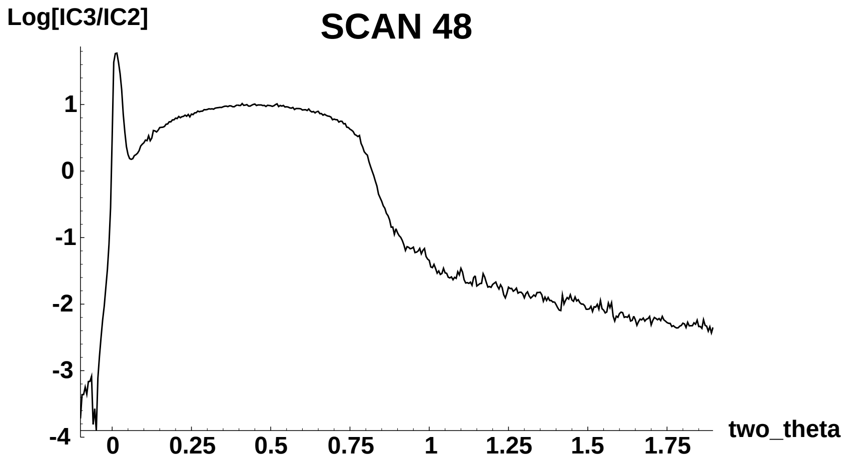

The procedure is exactly the same as for the unannealed film 13C. The geometric correction for the beam footprint is applied first. Then the theoretical reflectivity for a smooth niobium surface is divided out. The angles above $\alpha \approx 0.44$ degrees, which are dominated by diffuse reflection, are discussed later in the section on diffuse reflection below.

Upon making the same fit to a straight line (roughness form factor) as before, we obtain the result:

$$\sigma_{rough} = 20.82 \pm 0.15\ \AA \qquad log[B] = 2.234 \pm .006 \qquad B = 171 \tag{10}$$

Once again, the fit was made over the region $1 \leq 1000\ Q^2 \leq 3$. For the steep drop in the region above the critical angle, we obtain $\sigma(\alpha > \alpha_c) = 50.9\ \AA$. The final result shows the quality of the fit to 13D data:

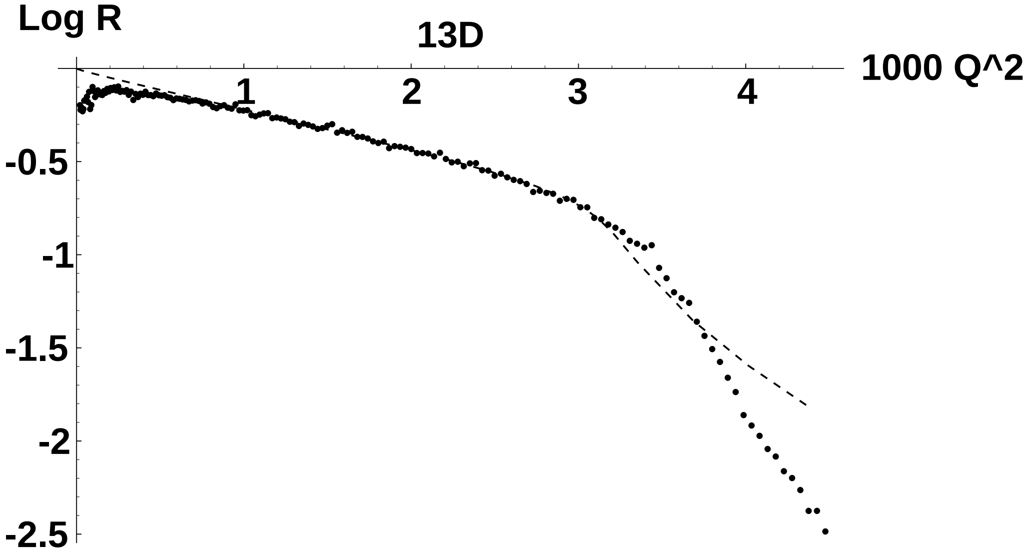

It appears that the data above the critical angle fits less well for 13D than for 13C. There may be a shift of α_c upward, indicating increased electronic density near the film surface. A more precise measurement could obtain interesting information about the film beyond the roughness measurement.

Conclusions Regarding the Specular Reflection From Niobium Films 13C and 13D

The change in beam size and Keithley gain make comparing the data from the two films a somewhat questionable procedure. However, the conclusion that annealing roughens the film, here only from an rms roughness of 18.8 Å to 20.8 Å, is probably correct. It is interesting also that the value of $\sigma_{\alpha>\alpha_c}$ actually *decreased* after annealing from 55 Å to 50.9 Å. Since we have not yet found a theoretical treatment appropriate for this case, we can't make any strong conclusions here about what is happening in the interior of the film. However it is known that Bragg reflection lines are dramatically narrower after annealing, indicating an increase in crystallite size and lessening of the random variation in lattice spacing. This is probably due to removal of defects associated with hydrogen [17].

When it is better understood, this region and the transition from below the critical angle to above it may provide important information about the just-below-the-surface region of the film.

We can do nothing with the two values for Log[B], the absolute intensity, since we did not measure the actual gain of the Keithley on the different scales and did not take a "zero scan" for the film 13D data. It would be good to have this information in the future.

So far we have ignored the specular scattering, which dominates both films for $\alpha \geq 0.44$ degrees.

Diffuse Reflection From Films 13C and 13D

Diffuse reflection measures the "height-height correlation" [18, 19, 20], i.e. the correlation between surface heights at two different locations, averaged over the surface.

The results * are shown below:

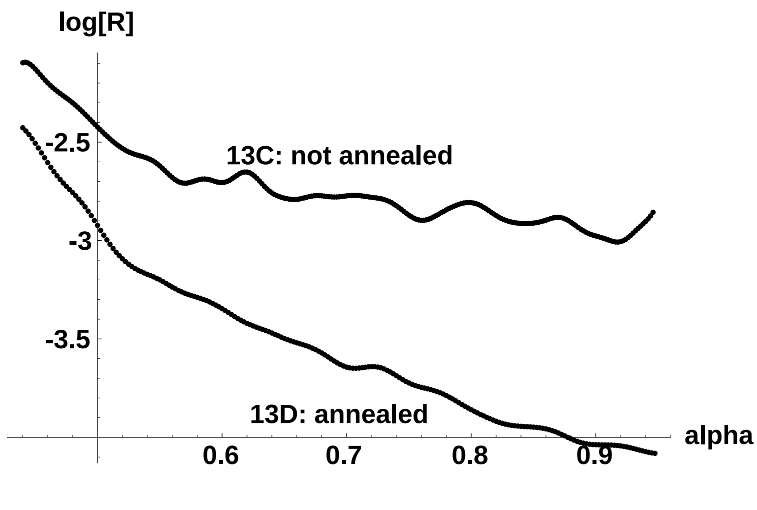

There are many caveats before this rather startling result can be believed. The data for 13D are taken

* Data gaussian smoothed with a sigma of .01 degree.

from the scan 48, which was also the source of the specular reflection data. The background subtraction can be believed here. Attempts on subsequent scans to focus on the large angle region did not give consistent results, something blatently obvious in the raw data. It may be due to attempts to zero the Keithley, etc., so we decided just to present data from the full scan. The 13C data, also from the full scan 38, which includes the specular data, scatter a great deal before the smoothing. The background subtraction is very questionable in the 13C data. If we compare the data taken before the peak, to the average for $2\theta > 1.5$ degrees, we get a signal/noise ratio of 1.27. The same number for 13D is 4.4. However, this may be overly pessimistic, since the counting rate just before the zero angle peak contains some amplifier "memory", etc, so may be an overestimate. The subtraction was based on the minimum number of counts, 96/sec. An independent measurement for 10 seconds gave 955, and 941 counts, so if anything we have slightly oversubtracted for the 13C data. In the case of 13D, the independent measurement, taken just before scan 48, and after the Keithley scale was changed, gave 1114 and 1142 counts/10 seconds. We subtracted a rate of 113 counts/second, based on the reading just before the peak, at negative values of 2θ .

The 13D data is of better quality in this angular region than the 13C data. This is in fact why we changed the Keithley gain after taking 13C.

These questions can be definitively resolved with an experiment designed to measure the diffuse scattering. We did more work on diffuse scattering on our A2 run, which we will report in a later paper.

Diffuse scattering is potentially an important and independent source of information.

Accepting provisionally and temporarily that annealing the film reduced the height-height correlation function, without an equally drastic change in $\sigma^2_{rough} \equiv < z^2 >$, what would this mean physically for the film surface? This question will be discussed further in the paper reporting the A2 run.

Finally, we can make a plot of log[R] vs. log[Q^2] for the more reliable data from film 13D.

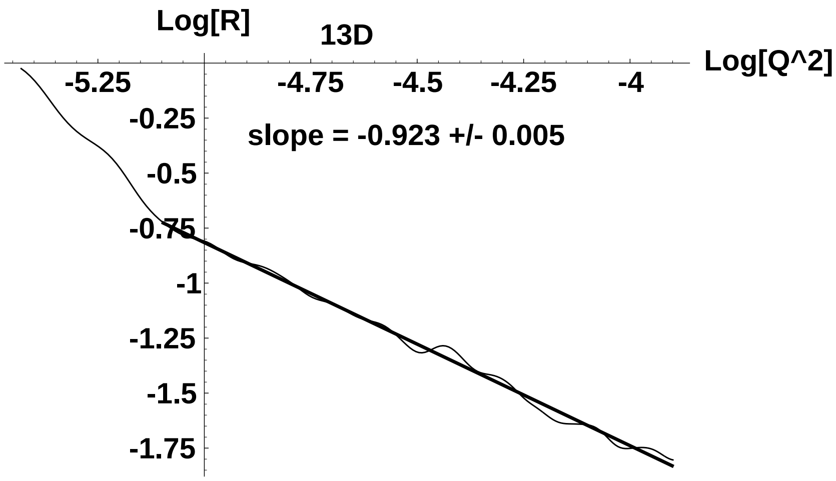

The straight line fit is $Log[R] = -5.432 \pm .022 - .923 \pm .005 Log[Q^2]$. (The errors are from a linear regression fit to a straight line.) We see that, over at least a decade, R fits a power law in Q^2 very well. Most theories of diffuse scattering predict $R \sim Q^{-(2+\epsilon)}$, where ϵ is a small positive number which contains specific information about the height-height correlation of the surface. We would need another experiment to show that this result of an exponent *less* than 2 in magnitude is actually correct, and to find the correct interpretation. More extensive, and much better quality experimental data is needed on diffuse scattering.

Overall Conclusions

We have demonstrated that precision measurements of niobium film surface roughness can be made at CHESS. The precision of these measurements can be still further improved by obvious experimental changes. Above the critical angle, there are some intriguing results which hint at new information about the below-surface structure of these films. Diffuse scattering is a topic which would also yield important information if the measurements were improved and transverse scans were included.

For an example of what can be done with more extensive measurements, read the reference [20] for detailed reconstruction of a Au(111) surface and vicunal surfaces of Si(111). (This is the paper immediately following the referenced theoretical paper by Held and Brock.)

The initial experiment has given us a good understanding of what is involved to obtain this information. We now need to correlate the x-ray data with superconducting measurements.

Acknowledgements

Dr. Randy Headrick of CHESS set up the F3 beam line for our use. Prof. Don Bilderback, Associate Director of CHESS provided key information about grazing angle x-ray scattering and many practical tips during the F3 run. We are greatly indebted for his help and moral support.

It is the use of the 1% monochromator which made these measurements possible, and which will be essential for future measurements.

This work made use of the Cornell Center for Materials Research Shared Experimental Facilities, supported through the National Science Foundation Materials Research Science and Engineering Centers program (DMR-9632275).

Special thanks are due to Gerhard Schmidt who prepared the films of TaN_2 and Nb, Ron Kemp who did the vacuum furnace annealing of sample 13D, and to Peter Revesz of the RBS Facility who did the RBS studies reported above.

Appendix I

Definition of Geometric Quantities

The necessary corrections to the data can be understood only by understanding the geometry in some detail.

We will assume that the x-ray beam is parallel to the x-z plane and is centered on the x axis. The positive z axis is in the vertical direction. The beam is assumed to be centered at the center of rotation. This is the origin of the coordinate system: x=y=z=0.

2θ is the angle through which the x-ray beam is scattered. The zero is defined by making a “zero scan” (see below).

The sample has a length L_s . The center of the sample is tilted at an angle α (not called θ here to avoid confusion, since it is independent of 2θ). The distance parallel to the sample surface, and along this surface will be called “u”. u ranges from -$\frac{L_s}{2}$ to $\frac{L_s}{2}$. The normal to the sample surface lies in the x-z plane. We do not here consider effects of sample tilting or curvature in the y-z plane.

The center of the sample (u=0) lies a distance “h” above the beam center, which is at z=0 by definition. In particular, h is not assumed to be exactly zero here.

The detector is located at a distance L from the origin. It is set at an angle 2θ in the x-z plane. The detector slits determine the acceptance of the detector. Define the vertical coordinate in the reference frame of the detector slit as “v”. v ranges from -$\frac{w_d}{2}$ to +$\frac{w_d}{2}$, if the slit vertical width is set to w_d . v=0 at the center of the slit.

An x-ray strikes the sample at position u. The z coordinate of this x-ray is, by definition, “t”.

$$\mathrm{t} = \mathrm{u}\ \sin(\alpha)\ +\ h\ \cos(\alpha) \tag{11}$$

. This ray may be specularly reflected to an angle 2α with respect to the beam. It strikes the detector slits at a certain v(u), defined as the difference between the center of the detector slit and the point on a circle of radius L at which the reflected x-ray strikes the plane of these slits. This function is easily derived, if we make the very good approximation that the reflected x-ray makes a right triangle with the tangent to the detector slit. It is:

$$\mathrm{v}(\mathrm{u};\alpha,\theta,\mathrm{h}) = \cos(2\theta)\ \left[\frac{\mathrm{u}'\sin(\alpha)\ -\ \mathrm{h}\cos(\alpha)\ +\ \mathrm{L}\sin(2\alpha-2\theta)}{\cos(2\alpha)}\right] \tag{12}$$

In a simplistic picture of the reflection geometry, $\alpha = \theta$ and h=0 if the sample is centered on the beam. In that case v $\approx$ t=u $\sin\theta$. Reflected rays will hit the slit in positions which correspond to their height t in the beam.

Three Types of Scans

It helps to define three different "scans" we can make with the goniometer. We give them names for mnemonic assistance.

1. *Zero Scan:* In this scan, the sample is removed, so that the direct beam can strike the detector. There are two possible configurations: wide detector slits (≈ 1 mm) to obtain the monitor/detector normalization, and narrow detector slits, width $\mathrm{w_d}$. 2θ is scanned, typically from -.05 to .05 degrees. Using the normalization from the wide slit scan, we obtain

$$\begin{aligned} I(2\theta = 0) &= \int dt\ G(t) \qquad \text{wide slit scan, flat top} \\ A_0 \equiv \int d(2\theta)\ I(2\theta) &= \int d(2\theta) \int dt\ G(t)\Theta_{det}(t - L2\theta) \qquad \text{narrow slits} \\ &= \frac{w_d}{L} \int dt\ G(t) \end{aligned} \tag{13}$$

   $G(t)$ is the beam intensity at height t. $\Theta_{det}(v)$ is the probability that an x-ray at position v with respect to the center of the detector slits will be detected. If there is no scattering or beam divergence, it is a function which is either zero or one. By making these two types of zero scan, we can measure the detector vertical slit width accurately. The nominal zero position for 2θ is also determined. Let A_0 be defined as the area under the peak for the zero scan with the detector slits set at $\mathrm{w_d}$.

2. *Triangle Scan:* For this scan, we mount the sample, adjusting the height to intercept half of the beam. (It is difficult to do this exactly.) The detector is placed at $2\theta = 0$ degrees, as determined by a zero scan. The tilt angle of the sample is varied over a range which, for our case, typically was ± 3 degrees. If the height is nearly correct, the intensity vs. α resembles a triangle, peaked at $\alpha = 0$. From the slopes of the two sides we can deduce the σ_{beam} (assuming it is a gaussian) and the displacement of the sample center dx. From the peak intensity compared to the zero scan, we deduce the actual sample height h, again assuming a gaussian beam. In principle, the actual beam shape could be learned from this scan, but there are some uncertainties concerning the definition of the sample edge.

$$I_\Delta(\alpha) \equiv I(\alpha, 2\theta = 0) \tag{14}$$

3. *Specular Scan:* This type of scan should have been done over the whole range of specular and diffuse scattering. In this experiment, we selected one angle for 2θ just below the nominal value of the critical angle and scanned over α. (Sometimes α was fixed, and 2θ varied instead.) If the reflection was specular, a peak was obtained. The calibration of α was done by assuming this peak occurred at $\alpha = \frac{1}{2}(2\theta)$. The peak resembled the zero scan, but was only half the rms width if α was the scan variable. We can calculate the area under the specular part of the peak:

$$A_{2\theta} \equiv \int d\alpha\ I(\alpha, 2\theta) = \text{fixed}) \tag{15}$$

The ratio below can be shown shown to equal:

$$\frac{2A_{2\theta}}{A_0} = R\ F\ \frac{B}{B_0} \tag{16}$$

R is the specular reflectivity at the angle selected, F is the fraction of the beam in the "footprint", which, with proper selection of slit widths should be close to 1. The ratio $\frac{B}{B_0} \leq 1$ is not usually included in equation (16). It represents that, for a given sample, not 100% of the beam would appear in the detector, even if $R = F = 1$. This may be due to pinholes or other defects in the sample, or perhaps a defocussing effect due to sample curvature, or other causes. It is independent of the calibration of the detector or monitor ion chambers, and should be a constant factor for all angles. Inclusion of this factor is only important if we want an independent verification of the normalization $\lim_{\alpha\to 0} R(\alpha) = 1$. B_0 is determined in the zero scan, and equals $\int dt\ G(t)$ as defined above.

The length of the sample determines the "footprint" of the beam on the sample. We will refer to the total length as $\mathrm{L_s}$.

In the case of reflected rays, we might also consider that the sample might be tilted into the y-z by a few tenths of a degree. This makes the problem three-dimensional. Imagine that you have a flat plane at height h. Position in this plane is given by (u+dx,y). Rotate the plane around the y axis by an angle α. Then rotate the plane around the x (beam) axis by an angle β. This is the tilt of the plane, which in one case was measured to be 0.2° . It is expected to be very small. The formula (12) above changes to

$$\begin{aligned}&\mathrm{v}(\mathrm{u};\alpha,\beta,\theta,\mathrm{h}) = \\ &\cos(2\theta)\frac{\mathrm{u}'\cos(\beta)\sin(\alpha)\ -\ \mathrm{h}\cos(\beta)\cos(\alpha)\ +\ \mathrm{L}\Big(-\sin^2(\frac{\beta}{2})\sin(2\alpha+2\theta)\ +\ \cos^2(\frac{\beta}{2})\sin(2\alpha-2\theta)\Big)}{\cos(2\alpha)}\end{aligned} \tag{17}$$

with the definition

$$\mathrm{u}' \equiv \mathrm{u} + \mathrm{dx} \tag{18}$$

If the beam has a finite lateral spread at the sample, we must add to (17) a term

$$\cos(2\theta)\ \ \sin(\beta)\ y \tag{19}$$

This term gives a tilt to the reflected line at the detector slits. "y" is averaged over the width of the beam at the sample, with the center being y=0.

The height in the beam at which the beam strikes the sample is

$$t = \cos(\beta)\sin(\alpha)\ \mathrm{u}'\ +\ \cos(\beta)\cos(\alpha)\ h\ +\ \sin(\beta)\ y \tag{20}$$

(17,19) reduce to (12) when $\beta = 0$. (20) reduces to (11).

Example of a Zero Scan

We can deduce a great deal of information about the beam by examining scans of this type with different slit widths. In particular, we cannot take the nominal slit widths as more than qualitative values, and instead must determine them from the data.

For example, we took a scan (52-0609) with the detector slits set at a nominal value of 1.0 mm, much wider than the beam width. The ratio $\frac{IC2}{IC1} = 0.249$ on this scan. Since IC2 was after the upstream slits, this gives a measure of their width.

The flat top of this trapezoidal distribution was 0.238 IC3 counts/IC2 count. This is essentially equal† to $\int G(\mathrm{t})\ \mathrm{dt}$. The integral under distribution was $A_0 = 0.0156$ IC3 counts*deg/IC2 count. From this, we deduce that

$$\frac{\mathrm{w_d}}{\mathrm{L}} = 1.144 \times 10^{-3}$$

From the 1.0 mm slit distribution, we can numerically differentiate it by taking differences. We obtain two peaks of opposite signs, which were well separated. The difference was also a measure of the ratio of detector slit width to the lever arm L:

$$\frac{\mathrm{w_d}}{\mathrm{L}} = 1.166 \times 10^{-3}$$

The ratios obtained differ by less than 2%. At the same time, we determined the center of the distribution to be at .00046 deg., essentially zero. The rms width of each peak, averaged over the two peaks is 7.45×10^{-3} degrees, which is 0.13 milliradians. This is a measure of the beam size in front of the detector slit.

Using the measured value of L=0.75±0.01 meters, we calculate the slit width $\mathrm{w_d}$ to be 860 microns in the first case, and 874 microns by the second method.

Next we turn to another zero scan (0609-21): both upstream monitor and detector slits were each set to nominal values of 250 microns. The ratio of IC2 counts to IC1 counts dropped 20% to 0.208 from 0.249. The integral $A_0 = 0.504 \times 10^{-4}$ radians times IC3 counts/IC2 counts. Using the value $\int G(\mathrm{t})\mathrm{dt} = 0.238$, we calculate that, in this case, $\frac{\mathrm{w_d}}{\mathrm{L}} = 2.12 \times 10^{-4}$, giving a detector slit width of 159 microns.

Next we examine the detailed shape of this scan to check our understanding. We vary the upstream slit setting to obtain the best fit to the data, with the detector slit assumed to be 159 microns. An additional gaussian is added in convolution with the two rectangular distributions.

$$\mathrm{w_m} = 167 \pm 2 \text{ microns} \qquad \mathrm{w_d} = 159 \text{ microns} \qquad \mathrm{L} = 0.75 \text{ meters}$$

† This number can differs from 1 for many reasons: different Keithley gains for IC3 and IC2, absorption in the approximately 1.5 meters of air, and perhaps a difference in the ion chambers' collection efficiency. See [21] for our evidence that air absorption is the principle factor.

The experimental result of the fit to this scan is shown as the points in the figure below (the abscissa units are 0.001 degrees, the ordinate counts in IC3/count in IC2):

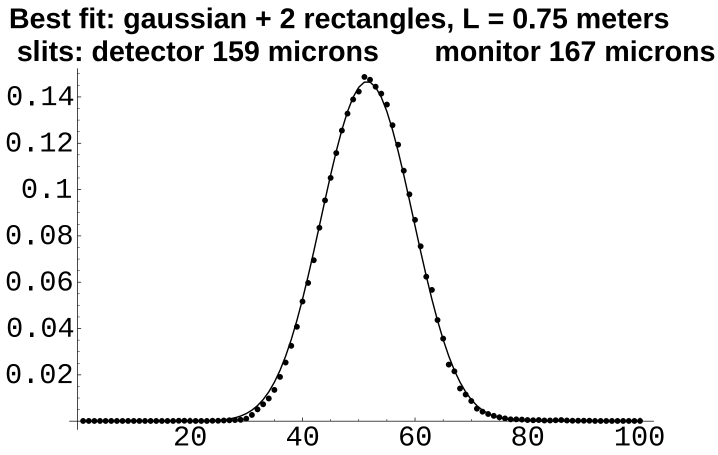

The rms width of the data points in the figure is $\sigma_{deg} = 7.87 \times 10^{-3}$ deg. Assuming Convolving two square distributions, the formula for $\sigma^2 = \frac{1}{12}\frac{\mathrm{w_m^2+w_d^2}}{\mathrm{L^2}}$. Using the values for the slit widths given above, we calculate that $\sigma = 5.1 \times 10^{-3}$ degrees, less than observed. An additional gaussian of rms width 6.0×10^{-3} degrees added in quadrature brings the rms up to the observed value. The fit depends only on a single parameter, the width of the upstream slit. The additional gaussian spread is possibly due to slit scattering from the monitor slits and/or air scattering in the path between the beam slits and the detector slits[21]. Assuming the distribution is a gaussian folded into two rectangular distributions, we can predict the distribution. This is the curve plotted above. The center of the experimental points lies at $2\theta = .0007$ degrees. A shift of this magnitude is readily seen and corrected.

To summarize the procedure we need to use for quantitative understanding:

1. From two zero scans, determine both the peak value and the area under the scan. The area determines the detector slit width $\mathrm{w_d}$, once $\int G(t)$ dt is known. One complication is that in the cases for which we have data, we did not take a type I scan with wide upstream slits ($\mathrm{w_m}$) in order to determine $\int G$. However, we can assume the scattering is now known, and only the two slit widths are unknown. We need an accurate beam distribution in order to determine the geometric and resolution corrections to the Berkeley reflectivity calculation.

2. From the triangular scan, we can determine the upstream beam shape, and the sample height and displacement from the center of rotation.

Taking the Data: Simultaneously Scanning $\alpha = \theta$ and 2θ

This is done to measure the reflectivity. When the angles are small, however, there is a contribution from the beam passing over the (tilted) sample and through the detector slits into IC3. Understanding the shape of this peak is a check on the understanding of the modelling.

We can write

$$I(\alpha = \theta, 2\theta) = \int_{\mathrm{h}+\left(\left(\frac{\mathrm{L_s}}{2}+dx\ \ Sign[\alpha]\right)\ |\sin\alpha|\right)} \mathrm{dt}\ G(\mathrm{t})\ \Theta(\mathrm{t}\ -\ 2\theta\ \mathrm{L}) \tag{21}$$

(We have approximated $\sin 2\theta$ by 2θ in the formula above.) Once we know $\mathrm{w_d}, \mathrm{w_m}$,h,dx,L for a given run or set of runs, this can be calculated in detail and compared with the results on the same runs for which reflectivity is measured.

An example of data taken under the same conditions as the data used for the scans 21-52 and 28-52 is the scan 41-53 in the figure below. The data are plotted on a log(base 10) plot vs 2θ in degrees. Data points are connected by lines drawn between the experimental points.

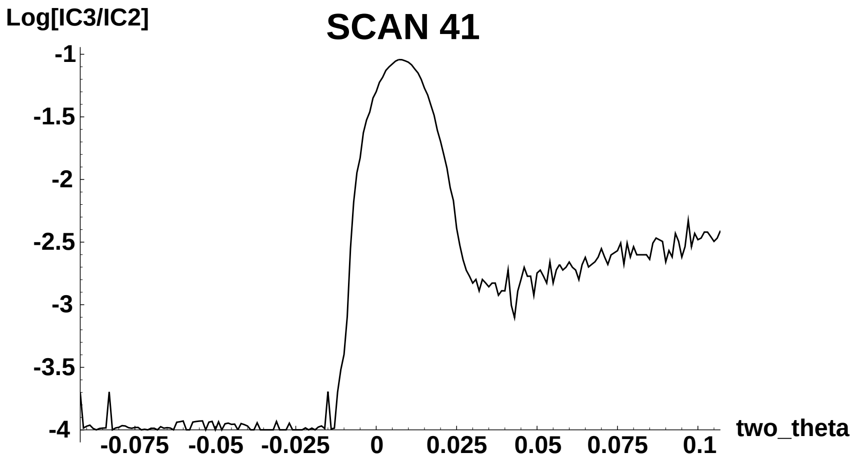

The same data can be plotted (as points) on a linear scale, and compared with the simulation.

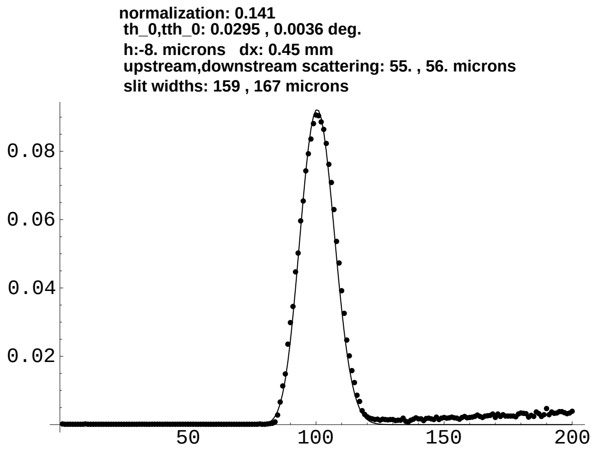

Most of the parameters, including the normalization, have been fixed by the zero scan of 21-51 and the triangle scan 28-52. Simulating the data above is very sensitive to the zero settings for 2θ and α, which are .0036 degrees and .0295 degrees respectively. A change in the zero of 2θ of .001 degrees is readily visible in the fit. What is seen in the solid line in the fit above is not necessarily the best fit, but is quite good, and determines the last parameters we need to calculate the geometric and resolution corrections to the theoretical reflectivity. In particular, the width of the curve fits well with no adjustable parameters which are determined in this I_3 type scan. A change in the sample height of even 1 micron has visible consequences. The result is $h = -8 \pm 1$ micron—astonishing accuracy. We have changed the displacement of the sample from the center of rotation to $dx = 0.45$ mm because the fit to the distribution 40-53 (an I_Δ scan not shown here) improved slightly over $dx = 0.5$ mm.

Corrections to the Reflectivity

On the right of the scan above can be seen the specular reflection at very small angles from the sapphire. We assume that we have available a theoretical calculation for $R(\alpha)$, taken from the Berkeley CXRO data. In the region $\alpha < 0.1$ degree, the reflectivity is nearly constant, equaling 0.9996 at $\alpha = .004$ degrees and .9918 at $\alpha = .100$ degrees. We assume an average R=0.995 for $\alpha \leq 0.1$ degrees.

The geometric corrections due to the changing footprint of the beam are changing rapidly, accounting for the nearly linear rise of the reflected intensity as seen in the figure above.

To calculate these corrections, introduce the variable u, which represents distance measured from the physical center of the sample surface. $-\frac{\mathrm{L_s}}{2} \leq u \leq \frac{\mathrm{L_s}}{2}$. The beam height is described by the variable t. We have, by geometry

$$\mathrm{t(u) = (u + dx)\ \sin\alpha\ +\ h} \qquad \alpha > 0 \tag{22}$$

$dt = \sin\alpha\ du$. Assuming specular reflection, the x-ray after reflection leaves the sample at an angle of 2α and enters the detector at a point v given by equation (12), with u in that equation replaced by u + dx, since we no longer assume the sample is centered on the center of rotation. The variable v is the distance from the center of the detector slit, which is located at 2θ L (for small angles).

The intensity is given by

$$I_{reflected}(\alpha) = \mathrm{R}(\alpha) \int_{\mathrm{t_{min}}}^{\mathrm{t_{max}}} G(t)\ \Theta(v(u(t);\alpha,2\theta))\ \ \mathrm{dt} \tag{23}$$

$\mathrm{t_{max}}, \mathrm{t_{min}}$ are found by setting $\mathrm{u} = \pm\frac{\mathrm{L_s}}{2}$ in (22) above.

The reflection part of the previous data (41-53) corresponds to $.01 \leq \alpha \leq .05$ degrees. After making all corrections, *using the same parameters* as for the fit to the direct beam illustrated in the previous figure, we take the ratio of the calculated intensity for $\mathrm{R}(\alpha) = 1$ to the observed intensity. This is illustrated below. The abscissa is α in degrees. (11,12) have been used to calculate the beam footprint, and the location of the reflected beam relative to the detector slits.

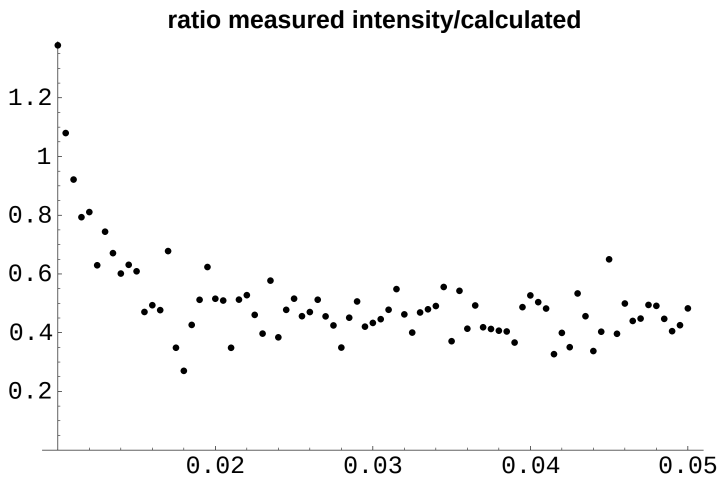

This is a surprising result. The correction flattens out data which rises about a factor of 3 between $\alpha = .02$ degrees and $\alpha = .05$ degrees. But the ratio of observed to predicted reflectivity in that region is only $0.46 \pm .06$, only half what was expected. We do not know why this is true, but think this is actually the case. We will need to have the reflectivity as $\alpha \to 0$ be an adjustable parameter, to be fit to the experimental result. In other words, the normalization must be determined by fitting the data.

Appendix II

Suggestions for improving the quality of the data in the future

1. Controlling the beam size is the highest priority. We need to be able to determine the beam parameters on-line: the triangle scan and zero scans need on-line analysis. An alternative to this would be to use fixed slits. In the future, a 10 mm sample size implies 40 micron monitor and detector slits; a 25 mm sample size implies 100 microns for the vertical slit widths.

2. The 1% monochromator is a *sine qua non* for future runs. Typically, we used between 1% and 20% of this beam. We should do the calculations using the data from the runs reported here to ensure there is enough intensity to follow the reflectivity curve down six orders of magnitude. The necessary intensity should be known in advance. On the run reported here, we obtained about 10^{14} photons/sec in the monitor IC1, which was upstream of the final slits.

3. We need to have a "run sheet" on which we record the scans and other data needed to analyze our runs. Under battle conditions, it was too easy to forget a zero scan, for example, or not to follow standardized conditions. The notebook is far too cryptic when read weeks or months later. We cannot trust that we will do complete records during the run, and it would be good preparation to make up a form prior to running.

4. In keeping with the goal of reliable data over six orders of magnitude, we need to improve the detector so that the dark current is not a problem. We suggest a completely new detector, using a channel photomultiplier like the PerkinElmer CPM which claims six to eight orders of magnitude are possible. This implies also developing the necessary electronics. It is our impression that the ion chamber/Keithley amplifier combination now in place is definitely inadequate for this purpose, making more than four orders of magnitude marginal at best, due to dark current instablity and the difficulty of zeroing the dark current. We should take the responsibility for doing this and integrating it with the F3 setup, where it could become a permanent feature of that beam line.

5. If possible, something should be done about the long path in air. 1.5 meters of air is a factor of 4 absorption at 8.5 KeV. There is also some scattering which reduces our resolution. Helium is the answer, but the logistics of doing this may prove difficult. This is probably a problem to be solved by CHESS.

6. We hardly measured the diffuse scattering at all. A precision measurement to determine the scaling exponent $R \sim Q^n$ to much better precision than was done here would yield new information about the surface. In order to measure the diffuse scattering we need a few points at large angles in which good statistics transverse scans in $\alpha \neq \theta$ are taken.

REFERENCES

[1] The surface and below surface NbO_x oxides have been shown by Halbritter to play an important role in the rf surface resistance at very low temperatures. But the degree and type of oxidation as a function of the parameters of film fabrication have not been systematically investigated, and films can vary widely, depending on whether columnar structure exists, whether they have been exposed to moist air, and other factors. References to this work by halbritter include: J.Halbritter, Appl.Phys. **A43**, 1 (1987), J. Halbritter, J. Less-Common Metals,**139**,133 (1988) and Electrochimica Acta **34**, 1153 (1989), J. Halbritter, Superconductivity **8**,691 (1995), J. Halbritter, Supercond. Sci. Technol. **12**, 883 (1999), J. Halbritter, Proc. 5 th Workshop on rf superconductivity, Hamburg, August 1991 (Ed. D. Proch, DESYM-92-01), p. 939 and Phys. Rev. bf B60,12505 (1999), J. Halbritter, Proc. **38** Eloisitron Workshop, Erice, Oct. 1999 (World Science Publ., 2000).

[2] *Non-uniformities in Hydrogen and Oxygen Concentration in Niobium Films*, W.R.Frisken, L.N.Hand, submitted to NIM B 2000. This describes work with imaging SIMS on a 2000 nm Nb film capped with 200 nm of Ti, and includes depth profiles of H, O and selected other elements. It also will be published in the near future as an SRF report.

[3] C.Benvenuti, S.Calatroni, I.E.Campisi, P.Darriulat, M.A.Peck, R.Russo, A.-M.Valente, *Study of the surface resistance of superconducting niobium films at 1.5 GHz*, Physica C **316**, 153(1999).

[4] *Handbook of Superconductivity*, edited by Charles P. Poole, Jr., Academic Press, 2000.

[5] In a very early paper (*Microwave Surface Resistance of Superconducting Niobium*, J.P.Turneaure,I.Weissman, Journal of Appl.Phys. **39**, 4417 (1968)) the authors conjectured that H_{c1} might be lowered by the accumulation of oxygen or carbon impurities near a grain boundary.They observe what they interpret to be flux penetration at $H_{rf} \approx \frac{H_{c1}}{4}$. This could be relevant to the segregation of oxygen with hydrogen observed by Frisken et al using imaging SIMS [2].

[6] R.Pöpel, *Electromagnetic Properties of Superconductors*, in the book *Superconducting Quantum Electronics*, edited by V.Kose, Springer-Verlag, 1989. The solutions of the Mattis-Bardeen equations for the BCS rf surface resistance are worked out in detail and compared to experimental results.

[7] D.H. Bilderback, *Reflecting Optics for Synchrotron Radiation*, Proceedings of SPIE, **v 315**, 90(1981) and D.C. Mancini, D.H. Bilderback *X-Ray Mirror Surfaces Evaluated By An X-Ray Topographical Techique*, CHESS Technical Memorandum No. 27, July 1982.

[8] The sapphire was a 10 mm x 10 mm x 0.5 mm A-cut ($11\bar{2}0$) substrate, "epitaxially polished". It was manufactured by the MarketTech International Corporation.

[9] A.Gibaud, G.Vignaud, S.K.Sinha,*The Correction of Geometrical Factors in the Analysis of X-ray*

Reflectivity, Acta Crystallographica, Section A, **49**, 642(1993).

[10] L.G. Parrett, *Surface Studies of Solids by Total Reflection of X-rays*, Phys.Rev. **v95**, 359(1954). This is a pioneering work which was ahead of its time. Parratt measured the oxidized lower density surface of copper, which was 25 years ahead of the same conclusion about niobium .

[11] δ and β are determined by the refractive index for x-rays, which is defined as $n_r \equiv 1 - \delta - i\beta$.

[12] We have used Parratt's formula 13, page 364 [10], which expresses the ratio of the half intensity angle to the critical angle as a function of $\frac{\beta}{\delta}$. In our case, $\frac{\beta}{\delta} = .01038$. The ratio of angles is 1.0143

[13] The numbers for δ, β have been scaled from the lower density assumed by Berkeley CXRO. There is some uncertainty in the actual density of our sample, and $2\theta_c$ may be the best way to determine the surface density. Berkeley calculations have been made for the lower density of 2.699 gm/cm^3, this means that it is difficult to make a quantitative comparison with the Berkeley reflectivity calculations. A step in this direction is taken when we scale everything in terms of $\frac{Q}{Q_c}$.

[14] The density of synthetic sapphire is listed as 3.97 gm/cm^3 in a brochure from the Saphikon, Inc., a leading producer of single crystal sapphire. It may also be calculated from the results in reference [16], which determined an electron density of $1.16 \pm .01 \times 10^(24)$ electrons/cm^3 from an x-ray reflectivity experiment. This implies a sapphire density of $3.928 \pm .034$ gm/cm^3. We have assumed this density in order to predict the critical angle. The handbooks list the density of $\gamma-$ corundum as 3.97 and $\alpha-$corundum as slightly higher than 3.97.

[15] We are indebted to Prof. Don Bilderback for bringing the existence of this important resource to our attention. The web address is "http://cindy.lbl.gov".

[16] A.Gibaud, R.A.Cowley, D.F. McMorrow, R.C.C. Ward, M.R. Wells, *High-resolution x-ray scattering study of the structure of niobium thin films on sapphire*, Phys. Rev. B, **v48**, 14463(1993).

[17] *Our Niobium Films Contain Hydrogen*, L.N.Hand,**SRF 000410-00**, April 10, 2000, and *Study of Annealing in Niobium Films*, L.N.Hand,R.H.Kapfer,W.R.Frisken,**SRF 000705-07**, July 5,2000

[18] R. Headrick, unpublished lecture notes (Cornell Physics 689), Spring 2000

[19] S.K. Sinha, E.B. Sirota, S. Garoff, and H.B.Stanley. *X-ray and neutron scattering from rough surfaces*, Phys. Rev. B, **v38**, 2297(1988)

[20] G.A.Held and J.D.Brock, *Calculation of x-ray-diffraction profiles from vicunal surfaces*, Phys.Rev B **51**,7262 (1995). This is a derivation of the Born approximation result for diffraction from a semi-infinite surface of arbitrary roughness and crystal structure. A nice piece of experimental work making use of "truncation rods" to study the surface reconstruction of Au(111) is A.R.Sandy, S.G.J.Mochrie, D.M.Zehner, K.G.Huang, Doon Gibbs, *Structure and phases of the Au(111) surface: X-ray scattering measurements*,Phys.Rev. B, **43**, 4667 (1991).

[21] From the Berkeley CXRO data, we calculate the attenuation length of STP air to be 1.166 meters for an x-ray photon energy of 8.5 KeV. The critical angle of scattering in nitrogen gas is 4.866×10^{-3} degrees, in oxygen 5.208×10^{-3} degrees, comparable to the empirical value of 6.0×10^{-3} which was necessary to fit the scan 21-57 data in the appendix. This highlights the necessary to use helium or vacuum in the path instead of air for precision small angle reflectivity measurements.